

Revisiting the matching of black hole tidal responses: a systematic study of relativistic and logarithmic corrections

Mikhail M. Ivanov,^{1a} Zihan Zhou^{2b}

^aSchool of Natural Sciences, Institute for Advanced Study, 1 Einstein Drive, Princeton, NJ 08540, USA

^bDepartment of Physics, Princeton University, Princeton, NJ 08540, USA

Abstract. The worldline effective field theory (EFT) gives a gauge-invariant definition of black hole conservative tidal responses (Love numbers), dissipation numbers, and their spin-0 and spin-1 analogs. In the first part of this paper we show how the EFT allows us to circumvent the source/response ambiguity without having to use the analytic continuation prescription. The source/response ambiguity appears if relativistic corrections to external sources overlap with the response. However, these corrections can be clearly identified and isolated using the EFT. We illustrate that by explicitly computing static one-point functions of various external fields perturbing the four-dimensional Schwarzschild geometry. Upon resumming all relevant Feynman diagrams, we find that the relativistic terms that may mimic the response actually vanish for static black holes. Thus, the extraction of Love numbers from matching the EFT and general relativity (GR) calculations is completely unambiguous, and it confirms previous results that the Love numbers vanish identically for all types of perturbations. We also study in detail another type of fine-tuning in the EFT, the absence of Love numbers' running. We show that logarithmic corrections to Love numbers do stem from individual loop diagrams in generic gauges, but cancel after all diagrams are summed over. In the particular cases of spin-0 and spin-2 fields the logarithms are completely absent if one uses the Kaluza-Klein metric decomposition. In the second part of the paper we compute frequency-dependent dissipative response contributions to the one-point functions using the Schwinger-Keldysh formalism. We extract black hole dissipation numbers by comparing the one-point functions in the EFT and GR. Our results are in perfect agreement with those obtained from a manifestly gauge-invariant matching of absorption cross sections.

¹ivanov@ias.edu

²zihanz@princeton.edu

Contents

1	Introduction and Main Results	1
2	Worldline EFT for Schwarzschild BHs	7
2.1	Perturbative General Relativity	7
2.2	Finite Size Effects	8
3	PN Corrections to External Fields: Generalities	14
3.1	Power Counting	14
3.2	EFT Diagrammatic Structure	15
3.3	EFT Diagrammatic Recurrence Relation	18
4	PN Corrections to External Fields: Explicit Calculations	20
4.1	Consistent Gauge	21
4.2	Spin-0/2	23
4.3	Non-Renormalization of Love Numbers	24
4.4	Spin-1 Electric Dipole	28
5	Black Hole Perturbation Theory	30
5.1	EFT versus the Frobenius Method	30
5.2	UV Calculation	32
5.3	Analytic Continuation	33
6	Dissipation Numbers	34
6.1	Near Horizon Teukolsky Equation	34
6.2	Dissipation Number Matching	36
6.3	On Cancellations of Dissipative Response in Advanced Coordinates	37
7	Conclusions and Outlook	38
A	Feynman Rules	39
B	Useful Mathematical Relations	41
B.1	(Spin-Weighted) Spherical Harmonics	41
B.2	Master Integrals	42
C	Reproducing Schwarzschild Metric at $O((m/r)^4)$	44
D	One-point Function of Spin-1 Electric Dipole	45

E	Teukolsky Equation in Schwarzschild BH	46
E.1	Equation In Different Coordinates	46
E.2	Matching Dissipation Number In Schwarzschild Coordinate	47
E.3	Comments on Maxwell-Newman-Penrose $\tilde{\Phi}_0$	48
F	Matching Dissipation Numbers From Amplitudes	49
F.1	Fluctuation-dissipation relation	49
F.2	Spin-2 Absorption Cross Section in the EFT	50

1 Introduction and Main Results

Background

The detection of gravitational wave signals with the LIGO/VIRGO interferometer have started the era of precision strong field gravity [1]. This remarkable experimental success has also motivated many new theoretical studies. One of the key parameters affecting the shape of the gravitational wave signal are tidal deformability coefficients, called Love numbers. In the context of neutron stars, the measurement of Love numbers offers a way to probe the neutron star equation of state [2–5]. As far as black holes (BHs) are concerned, their Love numbers have been found to vanish identically in four dimensions, which has interesting phenomenological and theoretical implications. In particular, Love numbers appear as Wilson coefficients in the point-particle worldline effective field theory. Hence, their vanishing implies a fine-tuning problem that is reminiscent of the notorious cosmological constant problem [6].

The effective field theory (EFT) of gravitational wave sources is a theoretical tool for systematic calculations of gravitational waveforms [7–12]. Within the EFT each compact object of an inspiraling binary is represented as an effective point particle. The finite-size structure is then captured by means of higher-derivative effective worldline couplings. This approach is similar to the multipole expansion in classical electrodynamics. The leading finite-size effects of compact objects are captured by worldline operators quadratic in curvature. The corresponding Wilson coefficients can be shown to reduce to “classical” Love numbers in the Newtonian limit. As mentioned above, the black hole Love numbers are zero, which means that the worldline EFT exhibits a strong fine-tuning when applied to black holes.

In four dimensions, the Love numbers were shown to vanish for both the Schwarzschild (static) [13–16] and rotating (Kerr) BHs [17–20]. The situation is more intricate for higher dimensional static BHs, where Love numbers can vanish, be order-one constant, or exhibit classical renormalization group running depending on the multipole index ℓ and the number of spacetime dimensions [16, 21]. This behavior is also quite unnatural from the perspective of Wilsonian naturalness. Importantly, spin-0 and spin-1 analogs of Love numbers also follow the same patterns as the spin-2 gravitational perturbations. This hints that the vanishing of Love numbers should have a general geometric origin. Recently, the naturalness paradox associated with the strange behavior of Love numbers has been addressed by a new symmetry of general relativity called the Love symmetry [22] (see [23, 24] for alternative proposals).

The literature on BH Love numbers is vast, but there are certain conceptual and technical difficulties that are yet to be addressed. Broadly, these are the problems with the definition of Love

numbers in general relativity, and the extraction of Love numbers from black hole perturbation theory (BHPT) calculations. The main goal of this paper is to show how these problems can be resolved in the worldline EFT approach. Let us describe these problems in more detail.

Definition of Love numbers in GR. Source/response ambiguity. Love numbers were originally defined in the context of Newtonian gravity. Imagine a nonrotating fluid star of mass M perturbed by an external tidal field of a small body. In the absence of the external perturbation the star would be spherical. The tidal forces, however, deform the star, and it acquires internal multipole moments I_L . The total gravitational potential around the star will look like [25]

$$\phi(\mathbf{x}) = \frac{M}{r} - \sum_{\ell=2} \left[\frac{(\ell-1)!}{\ell!} \mathcal{E}_L n^L r^\ell - \frac{(2\ell-1)!!}{\ell!} \frac{I_L n^L}{r^{\ell+1}} \right], \quad (1.1)$$

where \mathcal{E}_L are the multipole moments of the tidal potential, $L = i_1 \dots i_\ell$ is the multi-index, and $n^L = n^{i_1} \dots n^{i_\ell}$ is the tensor product of unit direction vectors $n^i = x^i/r$. In linear response theory the induced mass multipoles must be proportional to external perturbations, $I_L = -k_\ell R^{2\ell+1} \frac{(\ell-2)!}{(2\ell-1)!!} \mathcal{E}_L$, where R is the size of the star that we insert in accordance with dimensional analysis. The total potential then takes the form

$$\phi^{\text{pert.}}(\mathbf{x}) = - \sum_{\ell=2} \frac{(\ell-1)!}{\ell!} \mathcal{E}_L n^L r^\ell \left[\underbrace{1}_{\text{source}} + \underbrace{k_\ell \frac{R^{2\ell+1}}{r^{2\ell+1}}}_{\text{response}} \right], \quad (1.2)$$

where we have subtracted the monopole component. We stress that there is a clear separation between the source and response contributions in the Newtonian theory. The Love number is a coefficient in front of the $r^{-\ell-1}$ term in the Newtonian potential profile. Since we will be discussing BHs, we replace $R \rightarrow r_s$ (Schwarzschild radius) in what follows.

There are several ways to define the Love number in general relativity. Ideally, one wants a definition that would be gauge and coordinate invariant, and that would also reproduce Eq. (1.2) in the Newtonian limit. One common way is to extend the expression (1.2) to full general relativity. For instance, one may look at the temporal metric component $h_{00} = (g_{00} - 1)/2$ in the body's local asymptotic rest frame [26], which takes the following form [16]:

$$h_{00}^{\text{pert}}(\mathbf{x}) = \sum_{\ell=2} \frac{(\ell-1)!}{\ell!} \mathcal{E}_L n^L r^\ell \left[\underbrace{\left(1 + c_1 \left(\frac{r_s}{r} \right) + \dots \right)}_{\text{source}} + \underbrace{k_\ell \left(\frac{R}{r} \right)^{2\ell+1} \left(1 + b_1 \left(\frac{r_s}{r} \right) + \dots \right)}_{\text{response}} \right], \quad (1.3)$$

where c_1, b_1 are some calculable $\mathcal{O}(1)$ coefficients. The terms in the first line above represent post-Newtonian (PN) corrections¹ to the source generated by gravitational nonlinearity. We call them the “source series.” The second line above contains the response contribution plus PN corrections

¹Physically, we are interested in a situation when the external source is a companion object in the binary. In this case $\frac{r_s}{r} \sim v^2$ is a PN parameter. By this reason, we will call an expansion in r_s/r “Post-Newtonian” in this paper, although we never explicitly assume that the external source of tides and the BH are bound objects.

to it. We call them the “response series.” An obvious problem with the above definition is a possible ambiguity due to an overlap between the source and response series [16, 20, 27]. If this is the case, the coefficient in front of the $r^{-\ell-1}$ term in the generalized Newtonian potential is actually given by

$$\textcolor{red}{c}_{2\ell+1} + \textcolor{blue}{k}_{\ell m} . \quad (1.4)$$

Now it is not uniquely defined by the Love number. A popular way to get around this ambiguity is to do an analytic continuation for ℓ from the physical region $\ell \in \mathbb{N}$ to the unphysical region $\ell \in \mathbb{R}$ [16, 19, 20, 27]. This is motivated by the observation that for general noninteger ℓ the source and response series in Eq. (1.3) do not overlap. This is generically true for BH perturbations in a number of spacetime dimension greater than four [16]. Some physical interpretation of this procedure in four dimensions is given in Refs. [19, 20] in the context of the renormalized angular momentum [28–30]. The analytic continuation of the angular multipole number is, however, still an ad hoc prescription whose validity is not under rigorous theoretical control. In addition, the analytic continuation can work only when it is possible to obtain a closed perturbative solution for a generic ℓ . This may not be the case for some modified gravity theories, e.g., [31, 32]. This makes it desirable to develop a systematic and controlled approach that does not rely on the analytic continuation prescription.

Gauge invariance. The second problem with the definition (1.3) is that it is given in a particular coordinate system. Hence, it is not obvious that this definition is gauge invariant [33].

Logarithmic corrections. In principle, the functional form of the relevant field profiles can be more complicated than (1.3). In particular, there could be logs multiplying the $r^{-\ell-1}$ term [16, 20]. This additionally obscures the non-EFT definitions of the Love numbers.

Dissipation numbers. The final ambiguity associated with (1.3) is the interpretation of the coefficient in front of the $r^{-\ell-1}$ term. In general, the tidal response has conservative (time-reversal even) and dissipative (time-reversal odd) corrections. For Schwarzschild BHs this means that the total time-dependent response can be written as

$$k_\ell(\omega) \equiv k_\ell + i\nu_\ell r_s \omega + \mathcal{O}(r_s^2 \omega^2), \quad (1.5)$$

where ν_ℓ is the dissipation number (dissipative response coefficient) and ω is the frequency in the BH’s rest frame. In the Newtonian theory of fluid stars ν_ℓ is proportional to the fluid’s viscosity [25]. Note that this contribution vanishes in the static regime. The situation is more complicated in the case of Kerr black holes, where due to frame dragging, one needs to replace $\omega \rightarrow \omega - m\Omega$ (Ω and m being the angular velocity of the black hole horizon and the magnetic number, respectively), so that the dissipation is present even for static external sources [19, 20, 34]. This effect has caused some confusion in the previous literature; cf. [17–19, 27, 35, 36].

However, many of these ambiguities can be addressed within the context of worldline EFT [7–12]. In this theory, Love numbers as defined as Wilson coefficients of the static finite-size action

$$S_{\text{finite size}} = \sum_{\ell=2} \frac{\lambda_\ell}{2\ell!} \int d\tau E_{a_1 \dots a_\ell} E^{a_1 \dots a_\ell}, \quad (1.6)$$

$$E^{a_1 \dots a_\ell} = e_{\mu_1}^{a_1} \dots e_{\mu_\ell}^{a_\ell} \nabla^{\langle \mu_2} \dots \nabla^{\mu_\ell} C^{\mu_1 |\alpha| \mu_2 |\beta|} v_\alpha v_\beta,$$

where $C_{\mu\alpha\nu\beta}$ is the Weyl tensor, v^α is the point particle four-velocity, and e_μ^a are vectors defining a frame orthogonal to v^α . $\langle \dots \rangle$ denotes the procedure of symmetrization and subtracting traces.

In the definition (1.6) $E^{a_1 \cdots a_\ell}$ are multipole moments measured in the BH frame, $a = 1, 2, 3$ are the $SO(3)$ indices. One can perform a linear response calculation with the action (1.6) and find that upon identification $\lambda_\ell = (-1)^\ell r_s^{2\ell+1} k_\ell (\pi^{1/2} 2^\ell / \Gamma(1/2 - \ell))$, it precisely reproduces Eq. (1.2) in the Newtonian limit [20].

Within the EFT all gravitational corrections are computed as relativistic perturbations around the flat background [7, 37, 38]. In this regard the EFT is sometimes referred to as nonrelativistic general relativity. In this approach, the PN corrections in the source series of (1.3) are just classical nonlinear graviton corrections to the external source profile. These corrections, i.e., the coefficient $c_{2\ell+1}$, can be computed explicitly. After that the whole external field profile can be matched to a corresponding BHPT calculation. Therefore, the EFT allows us to get around the source/response ambiguity without having to use the analytic continuation of the multipole index.

To extract the Love numbers, one needs to match EFT and full general relativity (GR) (or BHPT) calculations. The cleanest way to do so is to compare two gauge-invariant observables, such as a cross section of the elastic scattering of gravitational waves off a BH geometry. For that one needs to know this cross section at least at the 5 post-Minkowskian (PM) order [7, 10].² However, there is a simpler way to obtain the Love numbers: one can match static graviton one-point functions such as (1.3). This procedure is delicate as it is done in a particular coordinate system.

To overcome possible issue with coordinate dependence, one needs to make sure that the one-point function calculations on both EFT and UV sides are carried out in consistent gauges. In this paper, we define an EFT gauge to be consistent with the background geometry if the background EFT one-point function of gravitons (i.e., without external fields) coincides with a perturbatively expanded full geometry. Once we have specified a consistent gauge, we can match the full one-point function including external perturbations, which will then give us the Love numbers. Since the EFT Wilson coefficients are universal, results would be gauge-independent even if some specific one-point functions are used for the matching are not.

As far as logarithmic corrections are concerned, they can easily be incorporated within the EFT and interpreted as a classical renormalization group (RG) running. In particular, the authors of [16] have carried out such a matching calculation for a scalar (dilaton) perturbation with a quadrupolar source. In this work, we build on the ideas of [16] and investigate the logarithmic running for a general multipolar index ℓ . As we discuss later, we also find some diagrams that were omitted in [16], and we argue why this did not affect their results. The authors of [16] also proposed a symmetry explanation of the absence of logarithmic running of Schwarzschild Love numbers in $D=4$, which we thoroughly scrutinize in our work.

Summary of Main Results

The result of this paper is summarized as follows.

- **Systematic study of PN corrections.**: We generalize the formalism of [16] by computing static one-point functions (profiles) of generic external fields perturbing the Schwarzschild

²See [39] for a recent discussion and simplifications in the context of the near/far zone factorization of the scattering amplitude.

geometry in the EFT. We carry out explicit calculations in terms of EFT Feynman diagrams for the electric-type (parity even) spin-0 and scalar graviton³ fluctuations in a general multipole sector ℓ . For the spin-1 case, we limit ourselves to the dipole sector $\ell = 1$. We show that in all these cases $c_{2\ell+1} = 0$, which implies that there is no mixing between the source and response contributions in the Schwarzschild background. By comparing our EFT expressions with the BHPT results, we confirm that the Schwarzschild BH Love numbers vanish identically. This is yet another confirmation of the gauge independence of the vanishing of Love numbers.

We have discovered a diagrammatic recurrence relation that has allowed us to resum all PN external source diagrams for a generic multipolar index ℓ . Our EFT diagrammatic recurrence relation matches the Frobenius series expansion of the relevant BHPT solutions. This allows us to completely reconstruct the BHPT results for one-point functions using the EFT. This extends and generalizes the result previously obtained in [16], which gave an EFT interpretation of the vanishing of quadrupole-type spin-0 Love numbers and their RG running.

- Detailed study of nonrenormalization of Love numbers:** With the Feynman diagram techniques mentioned above, we conduct a detailed analysis of logarithmic corrections to the Love numbers (i.e., their RG running). In the context of Wilsonian naturalness, one may expect that the classical RG running of Wilson coefficients should be a generic phenomenon. Indeed, we will confirm this expectation by showing that generic individual EFT loop corrections to the Love numbers do produce some logarithmic running for arbitrary gauge choices. However, the logarithms cancel once we sum over all loop diagrams. We interpret this miraculous cancellation as a consequence of the recently discovered Love symmetries [40]. For spin-0 and spin-2 perturbations the logarithmic corrections to Love numbers are completely absent if we use the Kaluza-Klein (KK) metric split [16, 37, 38] where there are no interaction vertices that could produce the logs. To the best of our knowledge, the absence of the RG running of Love numbers has not yet been explicitly demonstrated in the literature in full generality, although this fact is known in the EFT community [41–43] (see also [16] for the spin-0 quadrupole case results). Our results imply that the structure of perturbations in the isotropic KK gauge, or the apparent Z_2 symmetry for dilaton field $\phi \rightarrow -\phi$ [16], in fact *does not provide* a general IR symmetry explanation to the nonrenormalization of Love numbers. Rather, the KK split and the isotropic gauge simply appear as convenient tools to obtain this result in the particular cases of spin-0 and spin-2 fields. We demonstrate this explicitly in the case of spin-1 perturbations, which do not have the Z_2 dilaton symmetry, but whose worldline Wilson coefficient still possesses the nonrenormalization property. Working in the same isotropic KK gauge, we find that individual loop diagrams do produce log corrections to Love numbers, but these corrections cancel in an intricate manner when all contributions are summed together. This is a clear

³With some abuse of notation, we will refer to the scalar graviton (or dilaton, or the generalized Newtonian potential) field as a “spin-2 field.” This is because the Love number for the scalar graviton is the same as the Love number for the actual spin-2 metric field.

example showing that the Z_2 dilaton symmetry, in general, cannot be interpreted as an IR symmetry enforcing the nonrenormalization of Love numbers.

- **Off-shell matching of dissipation numbers:** We also study in detail the dissipative response of Schwarzschild black holes, especially, the off-shell 1-pt function matching, without using the analytic continuation techniques. In the EFT, the dissipation numbers are generated by internal degrees of freedom, which are encapsulated in composite mass multipole moments on the worldline [44]. In this paper we establish the explicit connection between this approach and the recent off-shell GR calculations of dissipation numbers in Refs. [19, 20]. To that end we compute the imaginary time-dependent part of the graviton one-point function using the Schwinger-Keldysh in-in approach [45–49] (also see [50–53] for reviews). In the EFT, this contribution is produced by the imaginary part of the retarded two-point correlator of composite mass multipole operators. With this calculation we confirm that the imaginary part of the coefficient in front of the $r^{-\ell-1}$ term (1.5) is indeed produced by the dissipation of the BH horizon. This helps resolve some confusion about the conservative and dissipative response terms, which was especially acute in the case of Kerr BHs [18, 27].

We explicitly match the dissipation numbers in the EFT and GR for spin-0, spin-1, and spin-2 external fields in a generic multipole sector. Unlike Refs. [19, 20], our results here do not rely on the analytic continuation prescription.

Our calculation explicitly demonstrates the equivalence of off-shell and on-shell extraction of dissipative responses: the dissipation numbers we extract from a graviton one-point function agree with the results of the matching at the level of the absorption cross sections [54, 55]. This serves as a consistency check of the EFT approach and solidly confirms interpretations of recent GR response function calculations [18–20, 27].

Outline

Our paper is structured as follows. We start with a recap of the nonrelativistic general relativity and the point-particle EFT in Section 2. Then we discuss the EFT diagrammatic structure and power counting rules in Section 3. There we show that logarithmic corrections to Love numbers are expected from the EFT, in general. In Section 4 we explicitly compute the scalar, photon, and scalar graviton static one-point functions in the EFT in the isotropic Kaluza-Klein gauge. For the spin-1 field we show that the logarithmic corrections actually cancel, while for the spin-0 and spin-2 cases the logs are actually not present at all in the isotropic Kaluza-Klein gauge. We also explicitly resum the spin-0, spin-2 dilaton and spin-1 dipole one-point functions in the EFT to all PN orders. In Section 5 we compute the same spin-0, spin-1, and spin-2 one-point functions and compare them with the EFT expressions. This way we establish that Love numbers vanish identically without any source/response ambiguity. In Section 6 we match the dissipation numbers by comparing the time-dependent one-point functions computed in the EFT and in BHPT. We draw conclusions in Section 7.

Some additional material is presented in several appendices. In Appendix A, we provide Feynman rules used in our diagrammatic EFT computation. In Appendix B we collect some useful mathematical relations. In Appendix C we show that our EFT setup correctly reproduces the

Schwarzschild metric perturbatively. In Appendix D we provide the details of the spin-1 electric dipole one-point function calculation. In Appendix E we derive the static spin-s Teukolsky equations in Schwarzschild coordinates and isotropic coordinates. We also show that the dissipation number is the same in both coordinates, which confirms its gauge invariance. Finally, in Appendix F we derive the dissipation-fluctuation relation for Schwarzschild BHs and compute the graviton absorption cross section in the EFT.

2 Worldline EFT for Schwarzschild BHs

In this section we introduce the EFT for Schwarzschild black holes in a long-wavelength tidal environment. We systematically describe the tidal response of a black hole to spin-0, spin-1, and spin-2 electric-type external perturbations. We start with a general EFT for GR in the Newtonian limit, and then we discuss an effective description of black holes. Importantly, we will show that the EFT clearly separates between the conservative and dissipative contributions.

2.1 Perturbative General Relativity

Let us consider gravity coupled to a source, which can be approximated as a point particle at leading order. They are described by the following action:

$$S = S_{\text{EH}} + S_{\text{pp}}, \quad (2.1)$$

where S_{EH} is the standard Einstein-Hilbert (EH) action, whilst S_{pp} is the point-particle action that depends on both the black hole worldline $x^\mu(\tau)$ and the metric,⁴

$$S_{\text{EH}} = -\frac{1}{16\pi} \int d^4x \sqrt{-g} R, \quad S_{\text{pp}} = -m \int d\tau \sqrt{\frac{dx^\mu}{d\tau} \frac{dx^\nu}{d\tau} g_{\mu\nu}}, \quad (2.2)$$

where τ is a worldline parameter. We also consider the bulk scalar and electromagnetic fields, which are described by the standard actions

$$S_\varphi = \frac{1}{2} \int d^4x \sqrt{-g} g^{\mu\nu} \partial_\mu \varphi \partial_\nu \varphi, \quad S_{\text{EM}} = -\frac{1}{4} \int d^4x \sqrt{-g} g^{\mu\nu} g^{\lambda\rho} F_{\mu\lambda} F_{\nu\rho}, \quad (2.3)$$

where $F_{\mu\nu} = \partial_\mu A_\nu - \partial_\nu A_\mu$. To reproduce a Schwarzschild black hole, we do not couple these test fields to our point mass. The black hole will still be affected by these fields through polarization effects.

We will use the “static gauge” choice for the worldline parameter $\tau = t$. We decompose the spin-0, spin-1, spin-2 fields, and the center of mass coordinate into the background part and long-wavelength fluctuating parts,

$$\begin{aligned} g_{\mu\nu} &= \eta_{\mu\nu} + h_{\mu\nu}, & \frac{dx^\mu}{dt} &= (1, v^i), \\ \varphi &= \bar{\varphi} + \delta\varphi, & A_\mu &= \bar{A}_\mu + \delta A_\mu. \end{aligned} \quad (2.4)$$

where $h_{\mu\nu}$, δA_μ , $\delta\varphi$ are fluctuations of the fields, and v^i is the point-particle spatial velocity component. In the rest frame of the BH (an equivalent of static gauge), the computation can be further simplified by setting $v^i = 0$.

⁴We work in a unit system where $\hbar = G = c = 1$.

Within the EFT both the background BH geometry and the fluctuations around it are computed perturbatively starting with a Minkowski background [7, 8, 10, 37, 38, 56]. To that end we expand the EH and the point particle actions over perturbations in $h_{\mu\nu}$, and solve them as an expansion in m/r in an appropriate gauge [7, 8, 57, 58]. The one-point function calculation of the metric field $h_{\mu\nu}$ perturbatively recovers the Schwarzschild metric. We perform this computation explicitly in Appendix C. Once we have recovered the Schwarzschild metric, we can consider fluctuations of the test spin- s fields ($s = 0, 1, 2$ here), and compute nonlinear, post-Newtonian corrections to their profiles. The actions (2.2), (2.3), however, do not capture finite-size effects of the black hole. We discuss them in detail now.

2.2 Finite Size Effects

To incorporate BH finite-size effects, such as responses to spin- s test fields, we use the approach of the point-particle EFT [8, 10, 20, 34, 44]. In the limit when the size of the body (R) is parametrically smaller than the wavelength of external perturbations, i.e., $|\vec{k}|R \ll 1$, conservative finite-size effects can be captured by a most general worldline action built out of long-distance degrees of freedom, i.e., long-wavelength test fields and the center of mass position x^μ , and satisfying symmetries of the problem. In the case of spherically symmetric spacetimes, such as Schwarzschild, these symmetries are the diffeomorphism invariance, gauge invariance for the Maxwell field, worldline reparametrization invariance, and local rotation symmetry. To explicitly realize these symmetries, it is convenient to use the four-velocity $v^\mu = \frac{dx^\mu}{d\tau}$, the covariant derivative along it, $D \equiv v^\mu \nabla_\mu$, and a set of tetrads e_a^μ carrying $SO(3)$ indices $a = 1, 2, 3$, and defining a frame orthogonal to v^μ . They satisfy $g_{\mu\nu} e_a^\mu e_b^\nu = \delta_{ab}$ and define the projector

$$P_{\mu\nu} = \delta_{ab} e_\mu^a e_\nu^b = g_{\mu\nu} + v^\mu v_\nu. \quad (2.5)$$

In what follows we will consider only the electric-type (parity-even) perturbations. Generalization to the magnetic (parity-odd) sector is straightforward. Note that thanks to the electric-magnetic duality of the Schwarzschild spacetime in four dimensions [59], the Love numbers for the magnetic perturbations must coincide with the electric ones [21]. Thus, for the purposes of our work it will be sufficient to consider the electric sector only.

We can use the above geometric objects to define field multipole moments,

$$E_L^{(s)} \equiv E_{\mu_1 \mu_2 \dots \mu_\ell}^{(s)} e_{\langle a_1}^{\mu_1} e_{a_2}^{\mu_2} \dots e_{a_\ell}^{\mu_\ell}, \quad (2.6)$$

where L denotes the multi-index a_1, a_2, \dots, a_n , and $\langle \dots \rangle$ denotes the symmetric trace-free (STF) part. Explicitly, we have

$$\begin{aligned} E_{a_1 \dots a_\ell}^{(s=0)} &= \nabla_{\langle a_1} \dots \nabla_{a_\ell} \varphi \\ E_{a_1 \dots a_\ell}^{(s=1)} &= \nabla_{\langle a_1} \dots \nabla_{a_{\ell-1}} E_{a_\ell} \rangle, \quad E_a = e_a^\mu v^\nu F_{\mu\nu} \\ E_{a_1 \dots a_\ell}^{(s=2)} &= \nabla_{\langle a_1} \dots \nabla_{a_{\ell-2}} E_{a_{\ell-1} a_\ell} \rangle, \quad E_{ab} = v^\alpha v^\mu e_a^\beta e_b^\nu C_{\alpha\beta\mu\nu}, \end{aligned} \quad (2.7)$$

where $C_{\alpha\beta\mu\nu}$ is the Weyl tensor. The effective action is naturally built from the fields' multipole moments $E_L^{(s)}$. In particular, the leading order (quadratic in perturbations) effective point-

particle action is given by:

$$\begin{aligned}
S_{\text{finite size}}^{(s) \text{ local}} &= \sum_{\ell} \frac{\lambda_{\ell}^{(s)}}{2\ell!} \int d\tau E^{(s)L}(x(\tau)) E^{(s)}_{L}(x(\tau)) \\
&+ \sum_{\ell} \frac{\lambda_{\ell(\omega^2)}^{(s)}}{2\ell!} \int d\tau DE^{(s)L}(x(\tau)) DE^{(s)}_{L}(x(\tau)) + \dots
\end{aligned} \tag{2.8}$$

As usual in the EFT, perturbation theory is organized in terms of the field strength and the derivative expansion. Note that since the theory is nonrelativistic, spatial and temporal derivatives in the body's rest frame enter effective operators on different footing; e.g., the first term in (2.8) does not have time derivatives at all. The frequency of the perturbation should also be smaller than the object's inverse size in order for the EFT to be valid, $\omega R \ll 1$. We will suppress the index (s) in what follows.

Note that due to isomorphism between the STF tensors and spherical harmonics [60], the number of indices in L corresponds to a multipole index ℓ ; i.e., $L = (a)$ describes the dipole (not present for spin-2 perturbations), $L = (a_1 a_2)$ describes the quadrupole, $L = (a_1 a_2 a_3)$ - the octupole moment, etc. The monopole moment ($\ell = 0$) may be present only for spin-0 fluctuations.

The local action (2.8) cannot reproduce absorption. To incorporate this effect we need to take into account unknown gapless degrees of freedom X on the worldline. To that end one introduces composite operators $Q_L(X)$ that correspond to body's multipole moments, including internal degrees of freedom. Then we add a new coupling between the composite internal moments Q_L and the long-wavelength tidal moments of perturbing fields E_L , which yield the following additional action [44]:

$$S_{\text{finite size}}^{(s)} = - \sum_{\ell} \int d\tau Q_L^{(s)}(X, \tau) E^{(s)L}(x(\tau)), \tag{2.9}$$

Although we do not know the explicit form of the operator Q_L , we can still analyze the structure of its correlation functions by making use of symmetry and parameterizing it with some unknown coefficients that are determined through matching to the UV theory. In general, correlation functions of Q_L contain both conservative and dissipative effects; i.e. they are nonlocal in time in general.

In this paper we focus on the matching of the one-point functions. Such a matching can be performed for different physical observables, i.e., correlation functions. In general, these correlation functions have to be of the Schwinger-Keldysh (in-in) type; i.e., the corresponding path integral has to satisfy the in-in boundary conditions. However, certain observables can be extracted from the usual in-out path integral; i.e., scattering amplitudes [61–66], conservative forces [67, 68] and the total radiated power [69, 70]. We will discuss this approach in detail shortly.

To compute the perturbative one-point function, we fix the retarded boundary condition when computing the Green function. This is equivalent to using the following linear response theory expression for Q_L ,

$$\langle Q_L(\tau) \rangle_{\text{in-in}} = \int d\tau' G_{\text{ret}L}^{L'}(\tau - \tau') E_{L'}(x(\tau')), \tag{2.10}$$

where we have introduced the retarded Green function,

$$G_{\text{ret}L}^{L'}(\tau - \tau') = i\langle [Q_L(\tau), Q^{L'}(\tau')] \rangle \theta(\tau - \tau'), \quad (2.11)$$

where $\theta(\tau)$ is the Heaviside step function. Since the retarded Green function in the complex frequency domain is analytic around $\omega = 0$, we can parametrize its Taylor expansion around the origin as [20, 34],

$$G_{\text{ret}L}^{L'}(\omega) = (\lambda_0^{\text{loc.}} + i\lambda_1^{\text{non-loc.}}(r_s\omega) + \lambda_2^{\text{loc.}}(r_s\omega)^2 + \dots)\delta_{\langle L' \rangle}^{(L)}, \quad (2.12)$$

where ... denote terms higher order in frequency and $\lambda_0^{\text{loc.}}$, $\lambda_1^{\text{non-loc.}}$, and $\lambda_2^{\text{loc.}}$ are free parameters (Wilson coefficients). They all have the dimensionality $\mathcal{O}(r_s^{2\ell+1})$. There are three comments in order.

- **Tensorial Structure.** The rotational symmetry of the Schwarzschild background dictates that the retarded Green function can only be an STF version of the Kronecker symbol.
- **Time Reversal Symmetry.** The terms with even and odd powers of frequency in the retarded Green function transform differently under time reversal. The part which is even under the exchange $\omega \rightarrow -\omega$ describes conservative effects, while the time-reversal odd part captures dissipation.
- **Locality.** The time-reversal invariant terms can be absorbed into local counterterms in the point-particle action (2.8). In this sense they just renormalize the Wilson coefficients that we already had in Eq. (2.8). In contrast, the time-reversal odd terms, cannot be recast into a local worldline action, and therefore we call them “nonlocal.”

It is instructive to compare Eq. (2.12) with the Feynman time-ordered Green function,

$$G_{\text{Fey}L}^{L'}(\tau - \tau') = \langle TQ_L(\tau)Q^{L'}(\tau') \rangle. \quad (2.13)$$

Its Fourier transform is symmetric under $\omega \rightarrow -\omega$ but not analytic around $\omega = 0$. The second relevant observation is that the Feynman and retarded Green functions are equivalent for conservative effects (i.e., off-shell modes) [10]. The third important observation is a variant of the fluctuation-dissipation theorem for static BHs [44],

$$\int_{-\infty}^{+\infty} d\tau e^{i\omega\tau} \langle Q_L(\tau)Q^{L'}(0) \rangle = 2\text{Im} \left(i \int_{-\infty}^{+\infty} d\tau e^{i\omega\tau} \langle TQ_L(\tau)Q^{L'}(0) \rangle \right), \quad (2.14)$$

valid for $\omega > 0$. All together, the above facts completely fix the form of the Feynman propagator in terms of the Wilson coefficients that we had in the EFT expansion of the retarded Green function. If we restrict the latter to the form (2.12), the Feynman propagator would take the form

$$G_{\text{Fey}L}^{L'}(\omega) = \left(-i\lambda_0^{\text{loc.}} + \lambda_1^{\text{non-loc.}}r_s|\omega| - i\lambda_2^{\text{loc.}}(r_s\omega)^2 + \dots \right) \delta_{\langle L' \rangle}^{(L)}. \quad (2.15)$$

The modulus of frequency next to the $\lambda_1^{\text{non-loc.}}$ term above explicitly reflects the nonanalyticity of the Feynman propagator at $\omega = 0$.

Love Numbers

Let us focus on conservative effects. It is instructive to start with the finite-size action Eq. (2.9), and use the standard EFT definition for the point-particle in-out effective action,

$$\exp\left(iS_{\text{eff}}^{\text{in-out}}(x^\mu, F)\right) \equiv \int \mathcal{D}X \, e^{iS[X, x^\mu, F]}, \quad (2.16)$$

where X is the unknown degrees of freedom on the worldline, and $F = (h_{\mu\nu}, A_\mu, \varphi)$ is the collective notation of long-wavelength probe fields. The effective action (2.16) results from integrating out all relevant short scale degrees of freedom plus the internal degrees of freedom X . We will suppress the explicit dependence on F in what follows. The leading order interaction term for a spin- s field for an individual orbital sector ℓ is given by

$$S_{\text{int}}^{\text{in-out}}(x) = \frac{i}{2} \int d\tau d\tau' \langle T Q_L(\tau) Q^{L'}(\tau') \rangle E^L(\tau) E_{L'}(\tau'). \quad (2.17)$$

In the static case it is sufficient to consider the $O(\omega^0)$ conservative part. After performing the Fourier transform, we get a local in time operator

$$\langle T Q_L(\tau) Q^{L'}(\tau') \rangle = -i\lambda_0^{\text{loc.}} \delta(\tau - \tau') \delta_{\langle L \rangle}^{L'}. \quad (2.18)$$

As anticipated, after plugging this into Eq. (2.17), we find that conservative effects can be captured by the local action

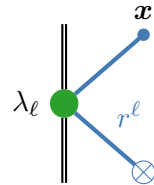
$$S_{\text{finite size}}^{\text{local}} = \frac{\lambda_\ell}{2\ell!} \int d\tau E_L E^L, \quad (2.19)$$

where $\lambda_\ell \equiv \ell! \lambda_0^{\text{loc.}}$. The Wilson coefficients λ_ℓ define static Love numbers in the point-particle EFT.

Let us focus now on the scalar-type Love numbers, for which $E_L = \partial_{\langle L \rangle} \varphi$. To extract the Love numbers, we decompose the profile φ into a background and fluctuation parts as in Eq. (2.4), and assume the background that solves the static bulk Klein-Gordon equation at $r \rightarrow \infty$,

$$\bar{\varphi} = \mathcal{E}_{i_1 \dots i_\ell} x^{i_1} \dots x^{i_\ell} \propto r^\ell Y_{\ell m}(\theta, \phi), \quad (2.20)$$

where $\mathcal{E}_{i_1 \dots i_\ell}$ is a constant tidal moments' tensor. Plugging this ansatz into the action Eq. (2.19), and taking into account the bulk scalar field action, we can perform a simple linear response calculation, whose diagrammatic representation is given below:



$$= \frac{(2\ell - 1)!!}{4\pi} \lambda_\ell \mathcal{E}_{i_1 \dots i_\ell} x^{i_1} \dots x^{i_\ell} \frac{1}{r^{2\ell+1}}. \quad (2.21)$$

Thus, we see that the Wilson coefficient λ_ℓ exactly coincides with the classic Love number in the Newtonian limit. The generalization to spin-1 and spin-2 perturbations is straightforward, and the corresponding Feynman rules are given in Appendix A, see also [20, 21].

Dissipation Numbers

The dissipation can be analyzed both within the in-out approach by matching to the total BH absorption cross section, or in the in-in formalism by matching to the frequency dependent one-point function of the external test field.

From the in-out formalism point of view, the $O(\omega)$ dissipative effect cannot be described by a local Lagrangian. Indeed, the term $\dot{E}_L E^L$ is a total derivative and thus can be removed from the Lagrangian⁵. To compute the cumulative power loss due to BH absorption, one can introduce a nonlocal in time action [44]. Indeed, plugging the Feynman Green function (2.15) into (2.9), we get:

$$S^{\text{diss.}} = \frac{i}{2} \int d\tau d\tau' \left(\int \frac{d\omega}{(2\pi)} \left(\lambda_1^{\text{non-loc.}} r_s |\omega| \right) e^{-i\omega(\tau-\tau')} \right) E_L(\tau) E^L(\tau'). \quad (2.22)$$

The parameter $\lambda_1^{\text{non-loc.}}$ can be determined from matching to the absorption cross section. For instance, the EFT absorption cross section in the sector $s = \ell$ is given by [44] (see Appendix F for a derivation in our unit system)

$$\sigma_{\text{abs, EFT}}^{(\ell=s)}(\omega) = 2^s \ell! \omega^{2s} r_s \lambda_1^{\text{non-loc.}}|_{s=\ell}. \quad (2.23)$$

Comparing this with the BH perturbation theory result in general relativity [54, 55],

$$\sigma_{\text{abs, GR}}^{(\ell=s)}(\omega) = \frac{8\pi(\ell+s)!2^s}{(2\ell+1)!!((2\ell-1)!!)^2 2^{2\ell+1}} r_s^2 (r_s \omega)^{2\ell}, \quad (2.24)$$

we obtain the following dissipation number

$$\lambda_1^{\text{non-loc.}}|_{s=\ell} = \frac{8\pi(\ell+s)!}{(2\ell+1)!!((2\ell-1)!!)^2 2^{2\ell+1} \ell!} r_s^{2\ell+1}. \quad (2.25)$$

Alternatively, the dissipation number can be read off from the one-point function of the external field computed within the Schwinger-Keldysh formalism. To that end, we compute the in-in effective action $\Gamma_{\text{eff}}^{\text{in-in}}$ defined through

$$\exp(i\Gamma_{\text{eff}}^{\text{in-in}}(\mathbf{x}_1, F_1; \mathbf{x}_2, F_1)) = \int \mathcal{D}X_1 \mathcal{D}X_2 e^{iS[X_1, x_1, F_1] - iS[X_2, x_2, F_2]}, \quad (2.26)$$

where \mathbf{x}_1 and \mathbf{x}_2 are the worldline coordinates and the subscripts 1, 2 denote forward and backward indices in the closed time path (CTP) (we follow the notation of [53]). The path integral here is done over two copies of the X field. All field satisfy the boundary condition $X_1 = X_2$, $F_1 = F_2$, and $\mathbf{x}_1 = \mathbf{x}_2 = \mathbf{x}_0$ at the final time slice $t = +\infty$ and the vacuum boundary condition at the initial time slice $t = -\infty$. We also use our freedom to choose \mathbf{x}_0 and place the BH at the origin. It is convenient to work in the Keldysh representation [48],

$$\begin{aligned} X_- &\equiv X_1 - X_2, & X_+ &\equiv \frac{1}{2}(X_1 + X_2), \\ F_- &\equiv F_1 - F_2, & F_+ &\equiv \frac{1}{2}(F_1 + F_2), \\ \mathbf{x}_- &\equiv \mathbf{x}_1 - \mathbf{x}_2, & \mathbf{x}_+ &\equiv \frac{1}{2}(\mathbf{x}_1 + \mathbf{x}_2). \end{aligned} \quad (2.27)$$

⁵More generally, all the terms involving odd number of derivatives are actually total derivatives and cannot be inserted into the local Lagrangian.

The 2×2 Green function of each field in $F = (h_{\mu\nu}, A_\mu, \varphi)$ is given by

$$G^{AB} = \begin{pmatrix} 0 & -iG_{\text{adv}} \\ -iG_{\text{ret}} & \frac{1}{2}G_{\text{H}} \end{pmatrix}, \quad (2.28)$$

where $A, B = \pm$, and G_{adv} , G_{H} are the advanced and Hadamard two-point functions respectively. The Feynman rules in the in-in formalism are very similar to those of the in-out formalism, but with contractions made over all closed time path indices A, B with the “effective metric”

$$c^{AB} = c_{AB} = \begin{pmatrix} 0 & 1 \\ 1 & 0 \end{pmatrix}, \quad (2.29)$$

Now we can write down the leading order interaction term in the in-in action,

$$\Gamma_{\text{int}}^{\text{in-in}}(\mathbf{x}_\pm, F_\pm) = \frac{i}{2} \int d\tau d\tau' \langle Q_L^A(\tau) Q^{L'B}(\tau') \rangle E_A^L(\tau) E_{L'B}(\tau'). \quad (2.30)$$

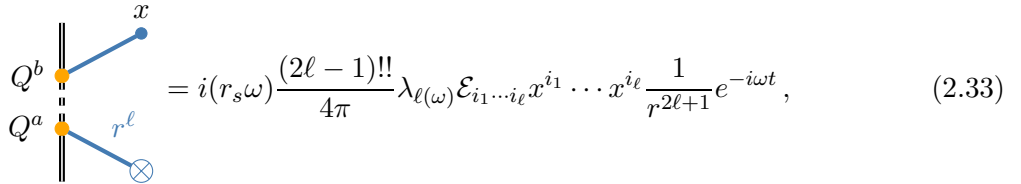
Now let us focus on the scalar field case, $F = \varphi$. To account for the external source component $\bar{\varphi}(\mathbf{x}, t)$, we choose $\bar{\varphi}_1 = \bar{\varphi}_2 = \bar{\varphi}$ so that $\bar{\varphi}_- = 0$, $\bar{\varphi}_+ = \bar{\varphi}$. It is now straightforward to compute the one-point function,

$$\begin{aligned} \langle \delta\varphi(\mathbf{x}, t) \rangle_{\text{in-in}} &= \int \mathcal{D}\delta\varphi_+ \mathcal{D}\delta\varphi_- \left(\delta\varphi_+(\mathbf{x}, t) e^{i\Gamma_{\text{int}}^{\text{in-in}}} e^{iS[\delta\varphi_1] - iS[\delta\varphi_2]} \right) \\ &\approx - \int dt_1 dt'_1 \langle Q^A(t_1) Q^B(t'_1) \rangle \partial^{(L)} \langle \delta\varphi_+(\mathbf{x}, t) \delta\varphi_A(\mathbf{x}_0, t_1) \rangle \partial_{(L)} \bar{\varphi}_B(t'_1) \\ &= \int dt_1 dt'_1 \langle Q(t_1) Q(t'_1) \rangle_{\text{ret}} \partial^{(L)} \langle \delta\varphi(\mathbf{x}, t) \delta\varphi(\mathbf{x}_0, t_1) \rangle_{\text{ret}} \partial_{(L)} \bar{\varphi}(t'_1). \end{aligned} \quad (2.31)$$

Let us compute now the dissipative contribution to the one-point function generated by the time-dependent generalization of the profile (2.20),

$$\bar{\varphi} = e^{-i\omega t} \mathcal{E}_{i_1 \dots i_\ell} x^{i_1} \dots x^{i_\ell}. \quad (2.32)$$

We insert this into Eq. (2.31), and use the static (instantaneous) propagator for $\delta\varphi$, which is sufficient to obtain the response at $\mathcal{O}(\omega)$. This calculation is almost identical to the above Love number calculation, and it can be represented by the following Feynman diagram:



$$= i(r_s \omega) \frac{(2\ell - 1)!!}{4\pi} \lambda_{\ell(\omega)} \mathcal{E}_{i_1 \dots i_\ell} x^{i_1} \dots x^{i_\ell} \frac{1}{r^{2\ell+1}} e^{-i\omega t}, \quad (2.33)$$

where we showed results in time-domain Fourier space. For future convenience, we have also redefined the coefficient $\lambda_1^{\text{non-loc.}}$ as

$$\lambda_{\ell(\omega)} = \ell! \lambda_1^{\text{non-loc.}}. \quad (2.34)$$

From (2.33), we explicitly see that the dissipation effect corresponds to the imaginary part of the one-point function of the external fields. The calculations for spin-1 and spin-2 perturbations are identical to the scalar field case, and the Feynman rules are given in Appendix A. We will perform an explicit matching to the UV theory in Section 6.

3 PN Corrections to External Fields: Generalities

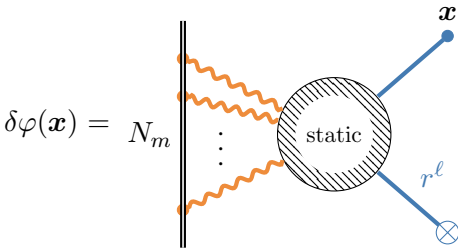
In the previous section we have introduced the BH response to external probes. If the external field profile has an asymptotic behavior $\propto r^\ell$ at spatial infinity, the response function would generate a correction to the field profile scaling as $\sim r^{-\ell-1}$. These corrections may be degenerate with the $2\ell + 1$ PN corrections to the source due to gravitational nonlinearities. Calculation of these corrections may be quite laborious given that GR is an effective theory with an infinite number of interaction vertices. In this section we show that this calculation is still possible thanks to a particular structure of the worldline EFT.

First, we introduce power counting rules and single out the relevant type of diagrams producing PN corrections. Second, we show that every such PN diagram can be presented as a “ladder” diagram built out of basic building blocks, which we call “pyramids.” This decomposition structure naturally leads to a recurrence relation between ladder diagrams of different PN order. In passing, we introduce an off-shell amplitude approach that allows us to estimate the momentum dependence of each PN diagram, which will be important for their future evaluation.

The discussion of this section is quite general, so we do not specify any gauge in GR calculations at the moment. For simplicity we focus on the case of the scalar test field profile here, although all results can be carried over to a general spin- s case. We do that explicitly in the next section.

3.1 Power Counting

The relevant small parameter in our discussion is the PN expansion parameter $m/r \ll 1$. The point-particle mass m is present only in the worldline point-particle action, so if we insert N_m point masses in our worldline we expect that it should modulate the static field profile by a factor $(m/r)^{N_m}$. We assume that the vacuum scalar field profile, i.e. in the absence of point masses and graviton, is simply equal to $\bar{\varphi}(\mathbf{x}) \propto r^\ell$. Then we are interested in diagrams which produce the following corrections,



$$\delta\varphi(\mathbf{x}) = N_m \left[\text{diagram} \right] \sim O \left(r^\ell \times \left(\frac{m}{r} \right)^{N_m} \right), \quad (3.1)$$

where the blob diagram inside is made of various GR vertices connected by propagators in the static limit.

The first relevant observation is that the scaling above is valid for *any* type of the blob diagram inside (3.1), provided that there are no quantum graviton loops. These loops are irrelevant in classical GR calculations that we do here and hence can be ignored.⁶ In general, the number of bulk quantum loops L_{Bulk} is given by

$$L_{\text{Bulk}} = P_h + P_{\delta\varphi} - V + 1, \quad (3.2)$$

⁶Note that in principle we can use the worldline EFT for quantum calculations as well.

where P_h is the number of corresponding bulk graviton propagators, $P_{\delta\varphi}$ is the number of $\delta\varphi$ propagators and V is the number of bulk vertices. Let us see now that $L_{\text{Bulk}} = 0$ ensures that the scaling (3.1) is always correct. Each propagator scales as $1/r$. Each bulk vertex scales as r since in gravity we only have the derivative couplings producing the $\int d^3x \partial\partial$ contribution. Now we can compute the total correction to the one-point function $\delta\varphi(\mathbf{x})$, from a diagram with N_m worldline point mass insertions, V vertices, P_h graviton propagators, and $P_{\delta\varphi}$ scalar propagators,

$$P_h + P_{\delta\varphi} - V + (N_m + 1) = L_{\text{Bulk}} + N_m = N_m , \quad (3.3)$$

where in the last equality above we used $L_{\text{Bulk}} = 0$.

Two comments are in order here. First, the power counting above does not capture logarithmic corrections, which can give rise to the renormalization group (RG) flow of Love numbers. In this sense it is appropriate to call it a “naive power counting.” Second, this power counting is gauge invariant, as it is based on the requirement that there are no quantum loops, which is clearly a gauge-independent statement.

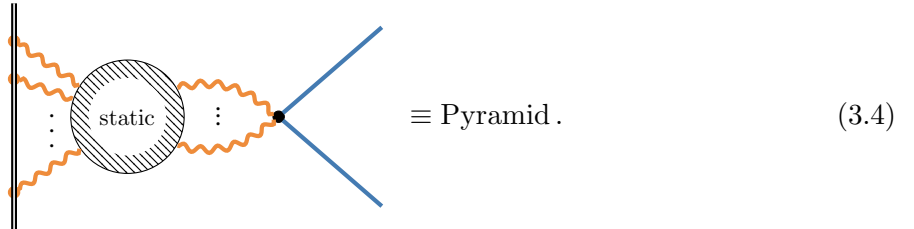
3.2 EFT Diagrammatic Structure

Let us discuss now the general form of the EFT worldline diagrams. We first show that each diagram has a typical “ladder” structure made of “pyramids.” These pyramid graphs are similar to the one-particle irreducible (1PI) diagrams because they cannot be reduced by cutting an external test field line. The 1PI diagrams are the simplest building blocks in our expansion. Any complicated “reducible” worldline graph can be presented as a product of these “1PI” diagrams.

It is also convenient to discuss diagrams assuming that the worldline is “amputated.” In this case each PN EFT diagrams can be thought of as an off-shell scattering amplitude.

Pyramids & Ladders

The basic building block in our diagrammatic expansion is a diagram that corresponds to an off-shell scattering process between a scalar and a gravitationally dressed worldline,



The above dots denote any number of graviton propagators that can be inside the diagram.

We call this diagram a “pyramid” because characteristic diagrams of this type have a pyramid shape. In what follows we use the term “connecting point” for the interaction vertex between $\varphi\varphi$ and bulk gravitons. We denote it with a black dot. Since we do not have quantum loops and the external source field cannot become virtual, the only diagrammatic structure compatible with bulk Feynman rules is the one where different pyramid graphs are connected to each other by scalar leg links between the connecting points. Such graphs are called “uncrossed ladder diagrams”⁷. Thus, a general PN diagram can be represented as a ladder graph made of pyramids,

⁷The crossed ladder diagrams are not possible in the static limit

$$(3.5)$$

Physically, this ladder structure has the interpretation that the gravitational nonlinear corrections to the source are generated by multiple scatterings between the off-shell scalars and gravitationally dressed point masses. As we will show shortly, the repetition of the same pyramid diagrams in a more complicated graph indicates that there should be a diagrammatic recurrence relation between corrections of different PN order.

Now, let us consider the pyramid diagram in detail. Starting from a single connecting point, diagrams connecting a scalar with the worldline have the following typical pyramid structure:

$$(3.6)$$

Power-Law Divergences

An important technical point is the presence of power-law divergences in our calculations. These divergences are unphysical and can be removed by local counterterms. The power-law divergences should be contrasted with logarithmic singularities, which have consequences on large scales and capture the physical effect of short modes that we have integrated out in the EFT.

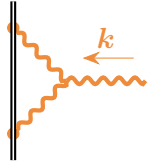
Let us first discuss the mass renormalization [37]. Naively, there are infinite many diagrams renormalizing the point mass that we need to compute even in the static case. However, we will see now that it is sufficient to ignore these diagrams and just replace the bare point-particle mass m with the physical renormalized BH mass M in all final answers.

The renormalized mass M is defined as the dressed 0-point function on the worldline,

$$(3.7)$$

Physically, this renormalized mass M can be viewed as the BH asymptotic Arnowitt-Deser-Misner (ADM) mass measured at the spatial infinity. Importantly, all loop corrections above lead to power-law divergences, and hence the presence of these diagrams does not change our power counting. These divergences can be absorbed into local counterterms. Thus, for all practical applications we can just first perform all calculations with the point particle bare mass m and then replace it with the physical renormalized mass M .

The second problematic aspect is the field strength renormalization of h . For example, if we assume a cutoff regularization, the following diagram would be linearly divergent:



$$\sim \frac{-i}{k^2} \Lambda + \text{finite term} . \quad (3.8)$$

In principle, the divergent part can be absorbed into the renormalized field strength h . We need to keep the physical finite part though as it produces a nonvanishing contribution to the amplitude.

An alternative option is to work in dimensional regularization, where all power-law divergences are automatically set to zero. This means, in particular, that there would be no difference between M and m . This is the approach that we will employ in what follows.

Off-shell Amplitudes

It is useful to focus on a blob diagram inside the pyramid and “amputate” the worldline and external scalar legs. This reduced blob diagram can be treated now as an off-shell amplitude. Let us estimate how this amplitude scales with external momentum in Fourier space. To that end we introduce N_m^{Pyr} , P_h^{Pyr} , N_h^{Pyr} and V^{Pyr} to denote the number of worldline vertices, bulk graviton propagators, external graviton legs, and the bulk vertices in a pyramid diagram, respectively.

The point mass contribution is a delta function in position space. Hence, each point mass leg scales as $|\mathbf{k}|^3$, giving a total momentum $|\mathbf{k}|^{3N_m^{\text{Pyr}}}$. Every graviton vertex $\sim \int d^3x \partial \partial$ has two derivatives, i.e., it scales as $|\mathbf{k}|^2$, giving a total of $|\mathbf{k}|^{2V^{\text{Pyr}}}$. All together, this gives a total number of momenta in the numerator $3N_m^{\text{Pyr}} + 2V^{\text{Pyr}}$. The momenta in the denominator come from static propagators $\sim k^{-2}$. Then the cumulative number of the momenta in the amplitude denominator from graviton propagators connecting point particles, scalar fields, and bulk vertices is $2(N_m^{\text{Pyr}} + N_h^{\text{Pyr}} + P_h^{\text{Pyr}})$. Note that the momenta flowing into our diagram from the connecting point must satisfy momentum conservation. The number of quantum loops in a pyramid diagram satisfies

$$L^{\text{Pyr}} = P_h^{\text{Pyr}} - V^{\text{Pyr}} + N_h^{\text{Pyr}} \equiv 0 . \quad (3.9)$$

Thus yields the total momentum scaling of an off-shell blob diagram

$$D = N_m^{\text{Pyr}} - 3 \quad (3.10)$$

Let us study now off-shell scattering amplitudes shown in Eq.(3.6). Recall that they serve as building blocks for our EFT one-point function calculation. From the symmetry perspective, this amplitude should be $\text{SO}(3)$ invariants. Suppose that the two external φ fields have momentum \mathbf{k}_1 and \mathbf{k}_2 . Then the amplitude of a generic pyramid diagram can only be a function of $|\mathbf{k}_1 + \mathbf{k}_2|$ and $\mathbf{k}_1 \cdot \mathbf{k}_2$. By using the momentum counting formula $D = N_m^{\text{Pyr}} - 3$ and taking into account two spatial derivatives acting on external φ legs, we get the following estimate the total amplitude:

$$\sim |\mathbf{k}_1 + \mathbf{k}_2|^{N_m^{\text{Pyr}}-3} (\mathbf{k}_1 \cdot \mathbf{k}_2) . \quad (3.11)$$

3.3 EFT Diagrammatic Recurrence Relation

As we discussed in Section 3.2, the ladder structure hints on a relationship between EFT PN diagrams of various orders. In other words, it suggests that higher order PN correction can be built from the lower order PN diagrams. Imagine that we want to compute the n PN correction to the scalar field profile $\delta\varphi^n$. It can be built from $(n-1)$ PN, $(n-2)$ PN, \dots by combining them with appropriate off-shell scattering amplitudes.

Suppose that we have a diagram made of two ladders. Each ladder has j_1 and j_2 mass insertions, respectively. This diagram can be represented as a product of two diagrammatic elements. The first one is a single ladder corresponding to a one-point function correction produced by j_1 mass insertions. The second element is an off-shell amplitude at j_2 PN order. We have

$$= \int \frac{d^3 \mathbf{k}_1}{(2\pi)^3} \int \frac{d^3 \mathbf{k}}{(2\pi)^3} \left(\text{Diagram 1} \right) \times \left(\text{Diagram 2} \right) \times \frac{-i}{k^2} e^{i\mathbf{k} \cdot \mathbf{x}} . \quad (3.12)$$

It is convenient to use the inverse Laplacian ∂^{-2} and the integration variable \mathbf{k}' defined as

$\mathbf{k} = \mathbf{k}' + \mathbf{k}_1$. Then the above integral can be rewritten as

$$\begin{aligned}
& \sim m^{j_2} \partial^{-2} \left[\left(\int \frac{d^3 \mathbf{k}_1}{(2\pi)^3} j_1 \left(\text{diagram with } \mathbf{k}_1 \text{ and } e^{i\mathbf{k}_1 \cdot \mathbf{x}} \right) \right) \cdot \left(\int \frac{d^3 \mathbf{k}'}{(2\pi)^3} \frac{\mathbf{k}'}{|\mathbf{k}'|^{3-j_2}} e^{i\mathbf{k}' \cdot \mathbf{x}} \right) \right. \\
& \quad \left. + \left(\int \frac{d^3 \mathbf{k}_1}{(2\pi)^3} j_1 \left(\text{diagram with } \mathbf{k}_1^2 \text{ and } e^{i\mathbf{k}_1 \cdot \mathbf{x}} \right) \right) \left(\int \frac{d^3 \mathbf{k}'}{(2\pi)^3} \frac{1}{|\mathbf{k}'|^{3-j_2}} e^{i\mathbf{k}' \cdot \mathbf{x}} \right) \right] \\
& = m^{j_2} \partial^{-2} \left[\left(\frac{j_2 x^i}{r^{j_2+2}} \partial_i - \frac{1}{r^{j_2}} \partial^2 \right) j_1 \left(\text{diagram with } \mathbf{k} \text{ and } e^{i\mathbf{k} \cdot \mathbf{x}} \right) \right]
\end{aligned} \tag{3.13}$$

Based on this factorization property, all higher order PN corrections can be constructed from lower order PN diagrams. Suppose that we want to compute an n PN correction $\delta\varphi^n(\mathbf{x})$. It can be built from a sum of all $(n-j)$ PN corrections $\delta\varphi^{n-j}(\mathbf{x})$ ($j = 0, 1 \dots n$) by combining them with the corresponding off-shell amplitudes

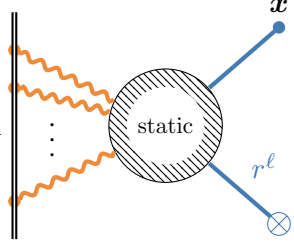
$$\begin{aligned}
\delta\varphi^n(\mathbf{x}) &= \sum_{j=1}^n \int \frac{d^3 \mathbf{k}_1}{(2\pi)^3} \int \frac{d^3 \mathbf{k}}{(2\pi)^3} \delta\varphi_{\mathbf{k}_1}^{n-j} \times \left(\sum_{\text{all possible diagrams}} j \left(\text{diagram with } \mathbf{k} \text{ and } e^{i\mathbf{k} \cdot \mathbf{x}} \right) \right) \times \frac{-i}{\mathbf{k}^2} e^{i\mathbf{k} \cdot \mathbf{x}} \\
&\sim \sum_{j=1}^n m^j \partial^{-2} \left(\frac{j x^i}{r^{j+2}} \partial_i \delta\varphi^{n-j}(\mathbf{x}) - \frac{1}{r^j} \partial^2 \delta\varphi^{n-j}(\mathbf{x}) \right),
\end{aligned} \tag{3.14}$$

where inside the large brackets we sum over all possible off-shell amplitudes with j worldline point mass vertices. Importantly, when the operator ∂^{-2} hits corrections scaling as $r^{-\ell-3}$, it gives rise to logarithmic divergences,

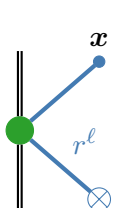
$$\partial^{-2} \left(r^\ell \times r^{-2\ell-3} Y_{\ell m}(\theta, \phi) \right) \sim r^\ell \times r^{-2\ell-1} \ln(r\mu) Y_{\ell m}(\theta, \phi), \tag{3.15}$$

where μ is the renormalization (momentum) scale (sliding scale). As we can see, the logarithmic divergences are generically present for each $2\ell+1$ PN order graph in an arbitrary gauge. But we

should notice that only the sum over all graphs is physical, which we denote by $c_{2\ell+1}$:

$$\sum_{\text{all possible diagrams}} 2\ell + 1 \times \text{static diagram} = c_{2\ell+1} \mathcal{E}_{i_1 \dots i_\ell} x^{i_1} \dots x^{i_\ell} \times \left(\frac{m}{r}\right)^{2\ell+1} \times \ln(r\mu) , \quad (3.16)$$


Physically, if $c_{2\ell+1} \neq 0$, the Love numbers will exhibit a running behavior. Indeed, the total term of order $r^{-\ell-1}$ in the test field profile is given by

$$\sum_{\text{all possible diagrams}} 2\ell + 1 \times \text{static diagram} + \lambda_\ell(\mu) \times \text{contact diagram} = \mathcal{E}_{i_1 \dots i_\ell} x^{i_1} \dots x^{i_\ell} \times \left(\frac{m}{r}\right)^{2\ell+1} \times \left(c_{2\ell+1} \ln(r\mu) + m^{-2\ell-1} \frac{(2\ell-1)!!}{4\pi} \lambda_\ell(\mu) \right) . \quad (3.17)$$


Since the physical one-point function should not depend on the renormalization scale μ , the Love number needs to flow with energy. The corresponding classical RG flow is given by

$$\mu \frac{d}{d\mu} \lambda_\ell(\mu) = -c_{2\ell+1} m^{2\ell+1} \frac{4\pi}{(2\ell-1)!!} . \quad (3.18)$$

We see that the condition of the absence of RG running for Love numbers is $c_{2\ell+1} = 0$. To determine $c_{2\ell+1}$, we have two ways. The first one is by summing over all the related EFT diagrams, and the second one is by matching to the UV theory to see whether there is any logarithmic terms. In the following sections, we will first give some specific examples of the EFT diagrammatic computations of the spin-1 dipole, and general spin-0 and spin-2 electric perturbations. These calculations indeed imply a vanishing $c_{2\ell+1}$. After that we will match the EFT and UV calculations, which confirm that the Love numbers indeed vanish.

4 PN Corrections to External Fields: Explicit Calculations

Let us demonstrate the general arguments given above on a concrete example. In this section we will explicitly compute $(2\ell+1)$ PN corrections to the spin-0,1,2 test field profiles. Our main result will be that the coefficient $c_{2\ell+1}$ vanishes for all types of perturbations. This means that the $(2\ell+1)$ PN corrections to the source terms vanish identically for Schwarzschild black holes, and hence Love numbers do not run. We prove that for a general orbital number ℓ in the case of spin-0 and spin-2 fields, and for the dipolar sector ($\ell = 1$) in the Maxwell field case.

4.1 Consistent Gauge

As a first step, we choose a convenient coordinate system. Since we are interested in the non-relativistic regime, it is customary to use the 3+1 metric decomposition based on the Kaluza-Klein reduction formula [16],

$$ds^2 = e^{2\phi}(dt - \mathcal{A}_i dx^i)^2 - e^{-2\phi}\gamma_{ij}dx^i dx^j, \quad (4.1)$$

where $\phi, \mathcal{A}_i, \gamma_{ij}$ is the Newtonian gravitational potential (dilaton field), the gravitomagnetic vector, and three-dimensional (3D) metric fields, respectively. They satisfy $\gamma^{ij}\gamma_{ik} \equiv \delta_k^j$ and $\mathcal{A}^i \equiv \gamma^{ij}\mathcal{A}_j$. The background field decomposition in this setup can be written as

$$\gamma_{ij} \equiv \delta_{ij} + \sigma_{ij}, \quad (4.2)$$

where σ_{ij} is the fluctuating part.

As a second step, we fix the gauge. This is an important aspect since all EFT and GR calculations, in practice, have to be carried out in a specific gauge (i.e., coordinate system). Ideally, one would want to match manifestly gauge-independent results, such as cross sections. In principle, one could also directly match one-point functions provided that they are computed in similar gauges. We formalize this statement by defining a notion of a “consistent gauge.” We call an EFT gauge consistent with the underlying GR background metric if the EFT calculation of the off-shell graviton one-point function reproduces the background metric perturbatively. The use of a consistent gauge ensures a correct matching between IR (EFT) and UV (GR) observables.

In practice, we choose a gauge that matches isotropic Schwarzschild coordinates. Recall that in these coordinates the BH solution takes the following form,

$$ds^2 = \left(\frac{1 - M/2r}{1 + M/2r} \right)^2 dt^2 - (1 + M/2r)^4 (dr^2 + r^2 d\Omega^2), \quad (4.3)$$

where M is the BH mass. From the EFT point of view, a gauge consistent with Eq. (4.3) can be fixed by the following requirements:

$$\sigma_{ij} = \sigma\delta_{ij}, \quad \mathcal{A}_i = 0. \quad (4.4)$$

In the static case, it is sufficient to consider off-shell potential modes for both external fields and GR degrees of freedom. There are no propagating degrees of freedom. Now let us expand the action in field perturbations. We have the following:

- Point particle term:

$$S_{\text{pp}} = \int dt \left(-m - m\phi - \frac{m\phi^2}{2} - \dots - \frac{m\phi^n}{n!} \right), \quad (4.5)$$

- Bulk graviton term: the EH action in the static limit takes the form

$$S_{\text{EH}} = -\frac{1}{16\pi} \int dt d^3\mathbf{x} \sqrt{\gamma} \left(-R[\gamma] + 2\gamma^{ij}\partial_i\phi\partial_j\phi - \frac{1}{4}e^{4\phi}\gamma^{ik}\gamma^{jl}\mathcal{F}_{ij}\mathcal{F}_{kl} \right), \quad (4.6)$$

where $R[\gamma]$ is the 3D Ricci scalar of γ_{ij} , and $\mathcal{F}_{ij} = \partial_i \mathcal{A}_j - \partial_j \mathcal{A}_i$. Perturbations in the isotropic gauge take the form

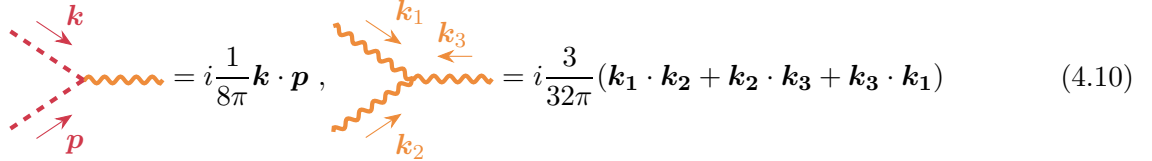
$$\begin{aligned} S_{\text{EH}}^{(2)} &= \frac{1}{8\pi} \int dt d^3 \mathbf{x} \left(-\partial_i \phi \partial^i \phi + \frac{1}{4} \partial_i \sigma \partial^i \sigma \right) , \\ S_{\text{EH}}^{(3)} &= \frac{1}{8\pi} \int dt d^3 \mathbf{x} \left(-\frac{3}{8} \sigma \partial_i \sigma \partial^i \sigma - \frac{1}{2} \sigma \partial_i \phi \partial^i \phi \right) , \\ &\dots\dots \end{aligned} \quad (4.7)$$

whilst the two-point correlation functions of ϕ and σ are given by

$$\langle \phi(\mathbf{x}_1) \phi(\mathbf{x}_2) \rangle = \text{---}\overset{\phi}{\text{---}}\text{---} = 4\pi \int \frac{d^3 \mathbf{k}}{(2\pi)^3} \frac{-i}{\mathbf{k}^2} e^{i\mathbf{k} \cdot (\mathbf{x}_1 - \mathbf{x}_2)} \propto \frac{1}{|\mathbf{x}_1 - \mathbf{x}_2|} , \quad (4.8)$$

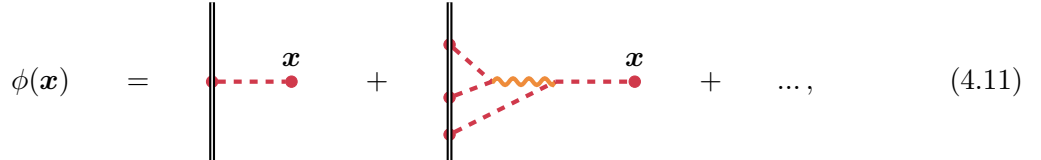
$$\langle \sigma(\mathbf{x}_1) \sigma(\mathbf{x}_2) \rangle = \text{~~~~}\overset{\sigma}{\text{~~~~}}\text{~~~~} = -16\pi \int \frac{d^3 \mathbf{k}}{(2\pi)^3} \frac{-i}{\mathbf{k}^2} e^{i\mathbf{k} \cdot (\mathbf{x}_1 - \mathbf{x}_2)} \propto \frac{1}{|\mathbf{x}_1 - \mathbf{x}_2|} . \quad (4.9)$$

Feynman rules for the above interactions are presented in Appendix A. For convenience, some of them are presented below:

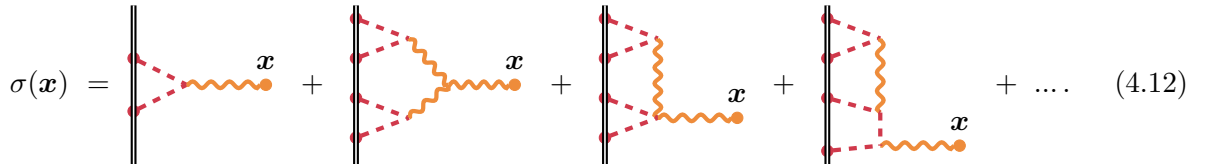


$$\begin{aligned} \text{---}\overset{k}{\text{---}}\text{---}\overset{p}{\text{---}}\text{---} \text{---}\overset{\sigma}{\text{~~~~}}\text{~~~~} &= i \frac{1}{8\pi} \mathbf{k} \cdot \mathbf{p} , \\ \text{~~~~}\overset{k_1}{\text{~~~~}}\text{~~~~}\overset{k_2}{\text{~~~~}}\text{~~~~}\overset{k_3}{\text{~~~~}}\text{~~~~} &= i \frac{3}{32\pi} (\mathbf{k}_1 \cdot \mathbf{k}_2 + \mathbf{k}_2 \cdot \mathbf{k}_3 + \mathbf{k}_3 \cdot \mathbf{k}_1) \end{aligned} \quad (4.10)$$

Now we can explicitly check that we reproduce the Schwarzschild metric in isotropic coordinates using our isotropic gauge; see Appendix C for more detail. Focusing on corrections up to $\mathcal{O}((m/r)^5)$, we get



$$\phi(\mathbf{x}) = \text{---}\text{---}\text{---}\overset{\mathbf{x}}{\bullet} + \text{---}\text{---}\text{---}\overset{\sigma}{\text{~~~~}}\text{~~~~}\overset{\mathbf{x}}{\bullet} + \dots , \quad (4.11)$$



$$\sigma(\mathbf{x}) = \text{~~~~}\text{~~~~}\text{~~~~}\overset{\mathbf{x}}{\bullet} + \text{~~~~}\text{~~~~}\text{~~~~}\overset{\sigma}{\text{~~~~}}\text{~~~~}\overset{\mathbf{x}}{\bullet} + \text{~~~~}\text{~~~~}\text{~~~~}\overset{\sigma}{\text{~~~~}}\text{~~~~}\overset{\mathbf{x}}{\bullet} + \dots . \quad (4.12)$$

Plugging these expressions into Eq. (4.1), we obtain

$$g_{00} = 1 - 2 \left(\frac{m}{r} \right) + 2 \left(\frac{m}{r} \right)^2 - \frac{3}{2} \left(\frac{m}{r} \right)^3 + \left(\frac{m}{r} \right)^4 + \mathcal{O} \left(\frac{m}{r} \right)^5 , \quad (4.13)$$

$$g_{ij} = \left(1 + 2 \left(\frac{m}{r} \right) + \frac{3}{2} \left(\frac{m}{r} \right)^2 + \frac{1}{2} \left(\frac{m}{r} \right)^3 + \frac{1}{16} \left(\frac{m}{r} \right)^4 + \mathcal{O} \left(\frac{m}{r} \right)^5 \right) \delta_{ij} . \quad (4.14)$$

After identification $m \rightarrow M$, we see that this metric coincides with the Schwarzschild metric in isotropic gauge (4.3) expanded up to $\mathcal{O}((m/r)^5)$. Thus, our isotropic KK gauge choices (4.1) and (4.4) are indeed consistent with the Schwarzschild metric.

In addition, let us point out that the commonly used de Donder gauge in the EFT is consistent with the harmonic Schwarzschild coordinates [57, 58]

$$ds^2 = \frac{r-M}{r+M} dt^2 - \frac{r+M}{r-M} dr^2 - (r+M)^2 d\Omega^2 . \quad (4.15)$$

4.2 Spin-0/2

We analyze now spin-0 and the spin-2 electric-type perturbations. These two types of perturbations share the same structure in the isotropic gauge, and hence it is natural to analyze them together. The bulk action for perturbations of a test scalar field Φ is given by

$$S_\Phi = -\frac{1}{2} \int dt d^3 \mathbf{x} \sqrt{\gamma} \gamma^{ij} \partial_i \Phi \partial_j \Phi . \quad (4.16)$$

The first important observation is that Φ only couples to the σ in the isotropic gauge, which significantly simplify our computations.

As far as the static spin-2 electric perturbations are concerned, we perform the following decomposition of the dilaton:

$$\phi = \phi_{\text{BH}} + \frac{\delta\phi}{2\sqrt{2}M_{\text{pl}}} , \quad (4.17)$$

where the Planck mass $M_{\text{pl}} \equiv 1/\sqrt{32\pi}$ in our unit system with $G = 1$. Physically, $\delta\phi$ is the perturbation of the Newtonian potential caused by an external metric fluctuation, while ϕ_{BH} is the background part that matches the Schwarzschild metric. Plugging this into the static Einstein-Hilbert action (4.6), we obtain the following effective action for $\delta\phi$

$$S_{\delta\phi} = -\frac{1}{2} \int dt d^3 \mathbf{x} \sqrt{\gamma} (\gamma^{ij} \partial_i \delta\phi \partial_j \delta\phi) , \quad (4.18)$$

which is the same as the scalar field action (4.16).

Now let us move on to the finite size effects. In the spin-2 case they are controlled by the electric tidal field related to the Weyl tensor. In the Newtonian limit, sufficient for the extraction of the finite-size effects from the worldline action, it is straightforward to get

$$E_{ij} \equiv 2\sqrt{2}M_{\text{pl}} C_{0i0j} = - \left(\partial_i \partial_j - \frac{1}{3} \delta_{ij} \partial^2 \right) \delta\phi , \quad (4.19)$$

where C_{0i0j} is the parity even component of the Weyl tensor.

Plugging this into (2.7) we find an expression for the static worldline action identical to that of the spin-0 case,

$$S_{\text{s}=0}^{\text{Love}} = \frac{1}{2\ell!} \int dt \lambda_\ell^{s=0} \partial_{\langle i_1 \dots i_\ell \rangle} \delta\phi \partial^{\langle i_1 \dots i_\ell \rangle} \delta\phi , \quad \text{cf.} \quad S_{\text{s}=2}^{\text{Love}} = \frac{1}{2\ell!} \int dt \lambda_\ell^{s=0} \partial_{\langle i_1 \dots i_\ell \rangle} \Phi \partial^{\langle i_1 \dots i_\ell \rangle} \Phi . \quad (4.20)$$

Since the spin-0 and electric spin-2 sectors are described by identical actions, we focus on the spin-0 case in what follows. Expanding in the number of fields and splitting each field component

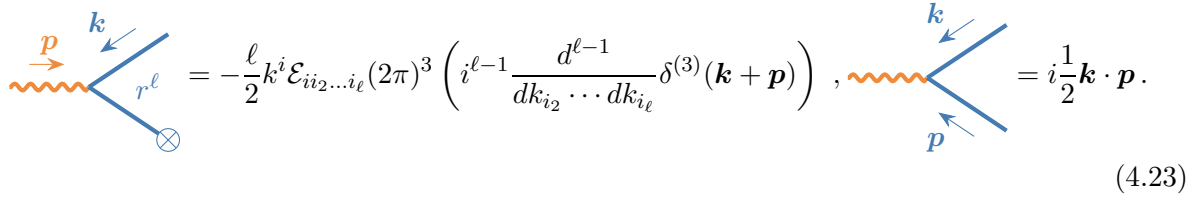
Φ into external source $\bar{\Phi}$ and response $\delta\Phi$, we obtain, at quartic order,

$$\begin{aligned} S_{\Phi}^{(2)} &= \int dt d^3\mathbf{x} \left(-\frac{1}{2}(\partial_i \delta\Phi \partial^i \delta\Phi) - (\partial_i \bar{\Phi} \partial^i \delta\Phi) \right), \\ S_{\Phi}^{(3)} &= \int dt d^3\mathbf{x} \left(-\frac{1}{4}\sigma(\partial_i \delta\Phi \partial^i \delta\Phi) - \frac{1}{2}\sigma(\partial_i \bar{\Phi} \partial^i \delta\Phi) \right), \\ S_{\Phi}^{(4)} &= \int dt d^3\mathbf{x} \left(\frac{1}{16}\sigma^2 \partial_i \delta\Phi \partial^i \delta\Phi + \frac{1}{8}\sigma^2 \partial_i \bar{\Phi} \partial^i \delta\Phi \right). \end{aligned} \quad (4.21)$$

The corresponding two point function takes the form

$$\langle \delta\Phi(\mathbf{x}_1) \delta\Phi(\mathbf{x}_2) \rangle = \frac{\delta\Phi}{(2\pi)^3 \mathbf{k}^2} e^{i\mathbf{k} \cdot (\mathbf{x}_1 - \mathbf{x}_2)} \propto \frac{1}{|\mathbf{x}_1 - \mathbf{x}_2|}. \quad (4.22)$$

Feynman rules for propagators and the above interaction vertices are given in Appendix A. The most important interaction vertices are



$$= -\frac{\ell}{2} k^i \mathcal{E}_{ii_2 \dots i_\ell} (2\pi)^3 \left(i^{\ell-1} \frac{d^{\ell-1}}{dk_{i_2} \dots dk_{i_\ell}} \delta^{(3)}(\mathbf{k} + \mathbf{p}) \right), \quad = i \frac{1}{2} \mathbf{k} \cdot \mathbf{p}. \quad (4.23)$$

4.3 Non-Renormalization of Love Numbers

Crucially, one may notice that the absence of Love numbers' running follow from the structure of metric perturbations in the isotropic Kaluza-Klein gauge. Indeed, in this gauge the point mass m couples to one ϕ , at leading order.⁸ The Einstein-Hilbert action (4.6), however, contains two ϕ 's; i.e., one can only have interactions such as $\phi^2\sigma$, $\phi^2\sigma^2$ etc. (we ignore derivatives here as they are irrelevant for our discussion). This means that it is only possible to draw a classical worldline diagram with an even number of ϕ 's and hence an even number of point masses. Therefore, it is impossible to construct a diagram producing a $(2\ell + 1)$ PN order correction to the one-point function, as this diagram obviously requires an odd number of point mass insertions on the worldline,⁹ $2\ell + 1$. Hence, $c_{2\ell+1} = 0$. This means that Love numbers do not get renormalized by graviton corrections. Recalling Eq. (3.18), this also implies that Love numbers do not run. Since Love numbers are defined as gauge-invariant EFT Wilson coefficients, the absence of their logarithmic running is a gauge-independent statement.

Note that the absence of logarithmic corrections does not follow from EFT power counting rules. Indeed, as we have mentioned earlier, in an arbitrary gauge one generally obtains non-trivial $(2\ell + 1)$ PN corrections from individual diagrams to the one-point function. Every such diagram would naively imply a logarithmic running. However, when summed together, these logs

⁸This order will be sufficient as diagrams with higher order interactions generate quantum loops and hence vanish in the classical limit.

⁹An equivalent argument was used by [16, 41, 42], which argue for the absence of logs by clashing the $\phi \rightarrow -\phi$ symmetry of the Einstein-Hilbert action in the isotropic Kaluza-Klein gauge and the $\phi \rightarrow -\phi$ to $m \rightarrow -m$ symmetry of the leading order point particle interaction.

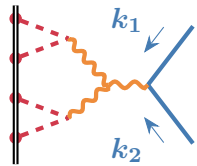
must cancel identically. From the EFT point of view, this cancellation is a fine-tuning, which is reminiscent of the apparent cancellation of loop corrections to the Higgs mass in the usual QFT.

Note that logarithmic contributions to Love numbers, if present, can be found in both the UV (full GR) and IR (EFT) calculations; see e.g., [16]. In Ref. [20] the absence of logarithmic running in four dimensions was interpreted as a constraint imposed by the Love symmetry of GR, which is a UV symmetry from the EFT point of view. Since the EFT must be a consistent description of the UV theory, the logs should be absent in the EFT as well. In an arbitrary gauge this appears as a miraculous cancellation between different Feynman diagrams. The choice of the isotropic gauge makes this cancellation manifest for spin-0 and spin-2 fields, but does not explain its origin. In this sense we cannot claim that the nonrenormalization of Love numbers is a consequence of some hidden structure of the GR action that is apparent in the isotropic gauge. As an explicit example supporting this statement, we will compute the running of the spin-1 Love number corrections shortly. We will see that in this case the isotropic gauge itself does not forbid Love numbers to run; i.e., individual $(2\ell+1)$ PN diagrams will contain logs as expected on general grounds. However, these contributions will sum to zero, implying the absence of running as enforced by the Love symmetry.

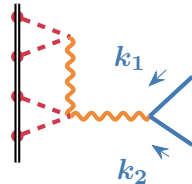
Reconstruction of the Full one-Point Function

Thanks to significant simplifications that take place in the isotropic gauge, we can actually compute PN corrections to the test field profiles to all PN orders. Let us show this explicitly.

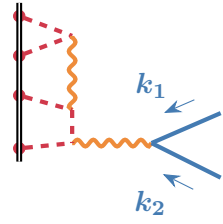
The first important observation is that all pyramid diagrams with more than two worldline point masses are unphysical and hence must exactly cancel with each other. Indeed, each pyramid diagram with N_m mass insertions scales as $|\mathbf{k}_1 + \mathbf{k}_2| N_m^{\text{Pyr}} - 3 (\mathbf{k}_1 \cdot \mathbf{k}_2)$ (3.11). Physical amplitudes should peak at the momentum conserving configurations $\mathbf{k}_1 + \mathbf{k}_2 = 0$ because the momenta of external legs do not change drastically in a soft scattering process characterized by $|\mathbf{k}|m \ll 1$. In contrast to this physical expectation, the amplitudes do not peak within the momentum conserving region if $N_m^{\text{Pyr}} \geq 4$. For these diagrams they peak when the momentum transfer is large, instead. Since this behaviour is clearly unphysical, the corresponding amplitudes must cancel with each other at any given order in m/r . To illustrate this argument explicitly, we provide a concrete example for the $N_m^{\text{Pyr}} = 4$ case. There are four possible diagrams in total:



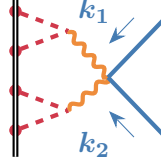
$$= (-i) \frac{1}{16} \pi^2 m^4 |\mathbf{k}_1 + \mathbf{k}_2| (\mathbf{k}_1 \cdot \mathbf{k}_2) , \quad (4.24)$$



$$= i \frac{1}{96} \pi^2 m^4 |\mathbf{k}_1 + \mathbf{k}_2| (\mathbf{k}_1 \cdot \mathbf{k}_2) , \quad (4.25)$$



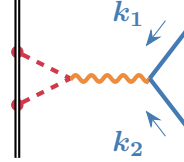
$$= i \frac{1}{48} \pi^2 m^4 |\mathbf{k}_1 + \mathbf{k}_2| (\mathbf{k}_1 \cdot \mathbf{k}_2) , \quad (4.26)$$



$$= i \frac{1}{32} \pi^2 m^4 |\mathbf{k}_1 + \mathbf{k}_2| (\mathbf{k}_1 \cdot \mathbf{k}_2) . \quad (4.27)$$

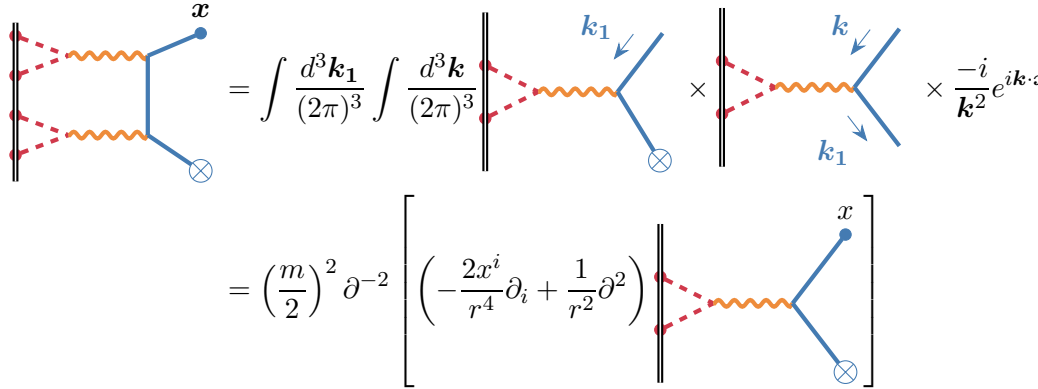
Obviously, these diagrams cancel when summed over. One can explicitly check that the same is true for any $N_m^{\text{1PI}} > 4$.

We conclude that only the amplitudes with $N_m^{\text{1PI}} = 2$ have the expected physical behavior. These amplitudes have poles in $|\mathbf{k}_1 + \mathbf{k}_2|$; i.e., they indeed peak at the momentum conserving region. This means that, in particular, the only diagram at leading order that is relevant for the pyramid structure is



$$= (-i) \frac{1}{2} (\pi^2 m^2) \frac{\mathbf{k}_1 \cdot \mathbf{k}_2}{|\mathbf{k}_1 + \mathbf{k}_2|} . \quad (4.28)$$

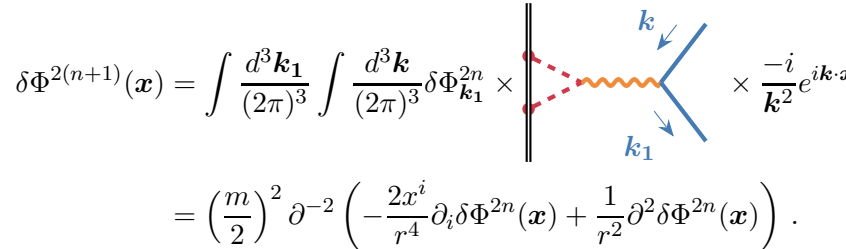
Knowing this diagram, we can compute the scalar field profile at all PN orders. In analogy with Eq.(3.12), we first establish the relation 4PN and 2PN corrections,



$$= \int \frac{d^3 \mathbf{k}_1}{(2\pi)^3} \int \frac{d^3 \mathbf{k}}{(2\pi)^3} \left[\text{diagram 1} \right] \times \left[\text{diagram 2} \right] \times \frac{-i}{k^2} e^{i\mathbf{k} \cdot \mathbf{x}} \quad (4.29)$$

$$= \left(\frac{m}{2} \right)^2 \partial^{-2} \left[\left(-\frac{2x^i}{r^4} \partial_i + \frac{1}{r^2} \partial^2 \right) \left[\text{diagram 3} \right] \right]$$

This expression can readily be generalized to an arbitrary $(2n)$ PN order,



$$\delta \Phi^{2(n+1)}(\mathbf{x}) = \int \frac{d^3 \mathbf{k}_1}{(2\pi)^3} \int \frac{d^3 \mathbf{k}}{(2\pi)^3} \delta \Phi_{\mathbf{k}_1}^{2n} \times \left[\text{diagram 4} \right] \times \frac{-i}{k^2} e^{i\mathbf{k} \cdot \mathbf{x}} \quad (4.30)$$

$$= \left(\frac{m}{2} \right)^2 \partial^{-2} \left(-\frac{2x^i}{r^4} \partial_i \delta \Phi^{2n}(\mathbf{x}) + \frac{1}{r^2} \partial^2 \delta \Phi^{2n}(\mathbf{x}) \right) .$$

Now let us assume an anzats

$$\delta\Phi^{2n}(\mathbf{x}) = \mathcal{E}_{i_1 \dots i_\ell} x^{i_1} \dots x^{i_\ell} \times c_{2n} \left(\frac{m}{2r}\right)^{2n}. \quad (4.31)$$

Then from Eq.(4.30) we obtain

$$\delta\Phi^{2(n+1)}(\mathbf{x}) = \mathcal{E}_{i_1 \dots i_\ell} x^{i_1} \dots x^{i_\ell} \times \left(\frac{(n-\ell)(2n+1)}{(n+1)(2n+1-2\ell)} c_{2n} \right) \times \left(\frac{m}{2r}\right)^{2(n+1)}, \quad (4.32)$$

implying the following recurrence relation for the PN coefficients c_{2n} :

$$c_{2(n+1)} = \frac{(n-\ell)(2n+1)}{(n+1)(2n+1-2\ell)} c_{2n}. \quad (4.33)$$

Note that the recurrence series truncates at $n = \ell$, which means that the static one-point function (in the absence of finite-size effects) is a polynomial in r . The truncation of the EFT solution can be seen as a fine-tuning. Indeed, this means that diagrams of $(\ell+1)$ PN order and higher all cancel identically. Equation (4.33) allows us to ‘resum’ PN corrections to all orders and obtain the full GR solution for the external field with a source boundary condition at spatial infinity,

$$\begin{aligned} \Phi(\mathbf{x}) &= \bar{\Phi}(\mathbf{x}) + \sum_{n=1}^{\infty} \delta\Phi^{2n}(\mathbf{x}) \\ &= \mathcal{E}_{i_1 \dots i_\ell} x^{i_1} \dots x^{i_\ell} \left(1 + c_2 \left(\frac{m}{2r}\right)^2 + c_4 \left(\frac{m}{2r}\right)^4 + \dots + c_{2n} \left(\frac{m}{2r}\right)^{2n} + \dots \right) \\ &= \sum_{m=-\ell}^{\ell} \mathcal{E}_{\ell m} Y_{\ell m}(\theta, \phi) r^\ell \left(1 + c_2 \left(\frac{m}{2r}\right)^2 + c_4 \left(\frac{m}{2r}\right)^4 + \dots + c_{2n} \left(\frac{m}{2r}\right)^{2n} + \dots \right), \end{aligned} \quad (4.34)$$

where the coefficients c_{2n} satisfy Eq. (4.33). One can easily identify this series with the Gauss hypergeometric function, giving

$$\Phi(\mathbf{x}) = \sum_{m=-\ell}^{\ell} \mathcal{E}_{\ell m} Y_{\ell m}(\theta, \phi) r^\ell {}_2F_1 \left(\frac{1}{2}, -\ell, \frac{1}{2} - \ell, \left(\frac{m}{2r}\right)^2 \right) \quad (4.35)$$

It is straightforward to write down an equation that is solved by this function,

$$R_\ell''(r) + \left(\frac{2}{2r-m} + \frac{2}{m+2r} \right) R_\ell'(r) - \frac{\ell(\ell+1)}{r^2} R_\ell(r) = 0. \quad (4.36)$$

Upon identification $m = M$ we see that this equation exactly coincides with the radial part of the Klein-Gordon equation in Schwarzschild isotropic coordinates, see Appendix E for more detail. The fact that we could completely reconstruct the Klein-Gordon equation even when we have ignored the finite-size effects suggests that Love numbers must be zero.

Towards Reconstructing the spin-2 Teukolsky Equation

As an additional consistency check, let us see if we can reproduce the spin-2 Teukolsky master equation. To that end we need to convert our metric perturbations into the Newman-Penrose

Weyl scalar. In the isotropic coordinates, the background Schwarzschild metric is given by (4.3). The Kinnersley tetrads read [71]

$$\begin{aligned} l^\mu &= \left(\frac{(M+2r)^2}{(M-2r)^2}, -\frac{4r^2}{M^2-4r^2}, 0, 0 \right), \quad n^\mu = \left(\frac{1}{2}, \frac{2(M-2r)r^2}{(M+2r)^3}, 0, 0 \right), \\ m^\mu &= \left(0, 0, \frac{2\sqrt{2}r}{(M+2r)^2}, \frac{i}{\sin\theta} \frac{2\sqrt{2}r}{(M+2r)^2} \right), \quad \bar{m}^\mu = \left(0, 0, \frac{2\sqrt{2}r}{(M+2r)^2}, -\frac{i}{\sin\theta} \frac{2\sqrt{2}r}{(M+2r)^2} \right). \end{aligned} \quad (4.37)$$

They satisfy $l^\mu n_\mu = 1, m^\mu \bar{m}_\mu = -1$. The Weyl scalar ψ_0 is defined as [72, 73]

$$\psi_0 = -C_{\mu\nu\alpha\beta} l^\mu m^\nu l^\alpha m^\beta. \quad (4.38)$$

Using the Kaluza-Klein decomposition Eq.(4.1), let us choose $\sigma = \sigma_{BH}$, $\phi = \phi_{BH} + \delta\phi/(2\sqrt{2}M_{\text{pl}})$ where σ_{BH} and ϕ_{BH} are determined by the background Schwarzschild metric, see Appendix C. Let us obtain now a linear perturbation equation for ψ_0 . In the Newtonian limit, the perturbed Weyl scalar ψ_0 is sourced by the Newtonian potential $\delta\phi$. Making use of the usual spin raising operator \eth^s (provided in Appendix B.1), we get the following expression in linear theory:

$$\psi_0 = 8\sqrt{2}M_{\text{pl}} \frac{r^2}{(M^2-4r^2)^2} \eth^1 \eth^0 \delta\phi \equiv \sum_{\ell=2}^{\infty} \sum_{m=-\ell}^{\ell} \mathcal{R}_\ell(r) {}_2Y_{\ell m}(\theta, \phi), \quad (4.39)$$

where ${}_2Y_{\ell m}(\theta, \phi)$ is the spin-2 spherical harmonics and $\mathcal{R}_\ell(r)$ is the radial part of ψ_0 . Recall now that $\delta\phi$ has the same description as a test scalar in the PN EFT. Hence, it also satisfies the Klein-Gordon equation (4.36). Acting on this equation with the spin raising operators and substituting $\mathcal{R}_\ell = R_\ell \frac{r^2}{(M^2-4r^2)^2}$ as dictated by Eq. (4.39), we obtain

$$\mathcal{R}_\ell''(r) + \left(-\frac{10}{M-2r} - \frac{4}{r} + \frac{10}{M+2r} \right) \mathcal{R}_\ell'(r) - \frac{-6+\ell+\ell^2}{r^2} \mathcal{R}_\ell(r) = 0. \quad (4.40)$$

We see that this equation reproduces the Teukolsky equation only up to subleading terms $O(\mathcal{R}_\ell M/r)$. This is because the full relativistic Weyl scalar ψ_0 is not completely determined by the Newtonian potential ϕ . It also depends on the metric perturbations $\delta\gamma_{ij}$ and the gravito-magnetic field δA_i . We have not included these perturbations because they do not affect the extraction of Love numbers from the one-point function matching. Indeed, for this purpose it is sufficient to use only ϕ . In principle, we could also perform matching at the level of the full Weyl scalar. In this case we would need to include fluctuations of $\delta\gamma_{ij}$ and δA_i components as well.

4.4 Spin-1 Electric Dipole

Let us now focus on spin-1 perturbations. The action for a Maxwell field in a curved spacetime is given by

$$S_{\text{EM}} = \int d^4x \sqrt{-g} \left(-\frac{1}{4} g^{\mu\alpha} g^{\nu\beta} (\partial_\mu A_\nu - \partial_\nu A_\mu) (\partial_\alpha A_\beta - \partial_\beta A_\alpha) \right). \quad (4.41)$$

where A_μ is the vector potential. The electric-magnetic duality of the Schwarzschild spacetime dictates that the spin-1 electric and magnetic Love numbers coincide. Hence, it will be sufficient to consider only the electric field, which is fully determined by the Coulomb potential, $E_i = -\partial_i A_0$.

This tells us that for the spin-1 electric dipole case $c_3 = 0$, which means that the spin-1 dipole polarization coefficients do not flow under RG (see Eq. (3.18)). Just like in the spin-0 and spin-2 examples, the absence of logarithmic running is fine-tuning from the worldline EFT perspective. Its origin can be traced to the Love symmetry in the UV [22].

Note that in contrast to the spin-0/2 cases, the isotropic gauge does not seem to be particularly useful for the spin-1 perturbations. As expected in the general case, here each PNEFT diagram carries a logarithm, which all cancel when all diagrams are summed together. We believe that there should exist a gauge where the cancellation of PN corrections to the spin-1 one-point functions is manifest to begin with. Since there are no logs in the UV theory, in such a gauge it should be possible to prove that $c_{2\ell+1} = 0$ for the electromagnetic (EM) perturbations for general ℓ . We leave an explicit construction of this gauge for future work.

5 Black Hole Perturbation Theory

To determine the Love numbers we need to match the full EFT calculation, including finite-size effects, to the UV theory result. The UV theory for our problem is the black hole linear perturbation theory. We will see now that one can match the EFT and UV expressions without any need for an analytic continuation. First, we will point out that the EFT calculation of the PN corrections to the source term is equivalent to constructing the solution with the Frobenius method. Then we will obtain spin-0,1,2 solutions in BH perturbation theory. Remarkably, these always coincide with the EFT solutions that describe external sources with PN corrections attached to them. Since the full solution is reproduced by the PN corrections alone, without any finite-size effects, the Love numbers must vanish identically.

Note that for the spin-1 and spin-2 perturbations we will match directly the Coulomb potential and the dilaton field profiles, respectively. These choices are gauge-dependent, but the results of our matching are not, as our EFT calculations are carried out in the gauges consistent with the background geometry and the gauge choice of the UV solution.

5.1 EFT versus the Frobenius Method

The Frobenius method is a method to construct a power series solution to a differential equation. We will see now that this power series exactly maps onto the PN diagrammatic method.

Let us start with the spin-0 case. For the spin-0 case, the corresponding Teukolsky equation is covariantly written as

$$\nabla_\mu \nabla^\mu \Phi(\mathbf{x}, t) = 0 . \quad (5.1)$$

Separating the variable as $\Phi(\mathbf{x}, t) = \sum_{\ell m} R_\ell(r) Y_{\ell m} e^{-i\omega t}$, we obtain the following equation for the radial function in the static limit:

$$R_\ell''(r) + \left(\frac{2}{2r - M} + \frac{2}{M + 2r} \right) R_\ell'(r) - \frac{\ell(\ell + 1)}{r^2} R_\ell(r) = 0 , \quad (5.2)$$

which is exactly the same as the equation obtained by the “resummation” of the EFT diagrams; see Eq. (4.36) with bare mass m replaced by BH mass M . The power series ansatz to solve (5.2) takes the form

$$R_\ell(r) = r^\ell \left(1 + c_1 \left(\frac{M}{2r} \right) + c_2 \left(\frac{M}{2r} \right)^2 + \cdots + c_{N_m} \left(\frac{M}{2r} \right)^{N_m} + \cdots \right) . \quad (5.3)$$

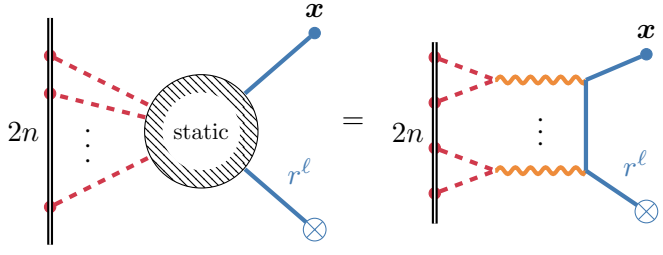
Note that this ansatz has an ambiguity for $N_m \geq 2\ell + 1$, which corresponds to a freedom of adding a decaying solution $\sim r^{-\ell-1}$ at $r \rightarrow \infty$. We will see in the next section that the series actually truncates at $N_m = \ell$. Plugging (5.3) into Eq. (5.2), it is straightforward to find that recurrence relation

$$(n+1)(2n+1-2\ell)c_{2(n+1)} = (2n+1)(n-\ell)c_{2n} , \quad (5.4)$$

which coincides with the EFT diagrammatic recurrence relation Eq. (4.33). This relation can be solved iteratively,

$$\begin{aligned} c_1 &= c_3 = \dots = c_{2\ell-1} = 0 , \\ c_2 &= \frac{\ell}{-1+2\ell} , c_4 = \frac{3(-1+\ell)\ell}{2(-3+2\ell)(-1+2\ell)} , \dots \\ c_{2n} &= (-1)^n \frac{(2n-1)!!}{2^n n!} (-n+1+\ell) \dots (-1+\ell)\ell \times \frac{\Gamma(\frac{1}{2}-\ell)}{\Gamma(\frac{2n+1}{2}-\ell)} , \quad n \leq \ell . \end{aligned} \quad (5.5)$$

Indeed, from the EFT diagrams we have:



$$\begin{aligned} &= r^\ell \times \left((-1)^n \frac{(2n-1)!!}{2^n n!} (-n+1+\ell) \dots (-1+\ell)\ell \frac{\Gamma(\frac{1}{2}-\ell)}{\Gamma(\frac{2n+1}{2}-\ell)} \right) \\ &\quad \times \left(\frac{m}{2r} \right)^{2n} , \end{aligned} \quad (5.6)$$

where we took into account only the physical pyramid graphs. The argument would be the same for static spin-2 electric perturbations captured by the dilaton field.

As far as the spin-1 perturbations are concerned, they satisfy the the covariant Maxwell equation

$$\nabla_\mu F^{\mu\nu} = 0 , \quad (5.7)$$

where $F_{\mu\nu} = \partial_\mu A_\nu - \partial_\nu A_\mu$. In the static case, the equation for A_0 and A_i decouple. Using $A_0(\mathbf{x}, t) = \sum_{\ell m} R_\ell(r) Y_{\ell m} e^{-i\omega t}$ and taking the static limit, we find

$$R_\ell''(r) + \left(\frac{2}{M-2r} + \frac{6}{M+2r} \right) R_\ell'(r) - \frac{\ell(\ell+1)}{r^2} R_\ell(r) = 0 . \quad (5.8)$$

Focusing on the dipole case, we can get the following coefficients with the Frobenius method:

$$c_1 = -2, \quad c_2 = 1 , \quad c_n, \quad n > 2 = 0 , \quad (5.9)$$

which coincides with the explicit EFT diagrammatic computation presented in Appendix D.

All in all, the upshot of this Section is that the EFT calculation of the PN corrections to the source has a one-to-one mapping onto the Frobenius method of solving field perturbations in the Schwarzschild background. The Frobenius method builds a solution in terms of a power series in m/r , attached to the growing source asymptotic r^ℓ . In our case this solution happened to be a polynomial, which is also regular at the BH horizon. By the uniqueness theorem, another linearly independent solution is singular at the horizon, and hence it does not contribute to the physical profile. In other words, the Frobenius solution is the full solution. The structure of this solution implies that the PN corrections to Love numbers and Love numbers vanish altogether.

5.2 UV Calculation

Spin-1

We seek a solution of the Maxwell equation (5.8) rewritten in a new variable $z = M/(2r)$,

$$R_\ell''(z) + \left(\frac{1}{1-z} + \frac{3}{1+z} \right) R_\ell'(z) - \frac{\ell(1+\ell)}{z^2} R_\ell(z) = 0 . \quad (5.10)$$

The above equation can be recast into the standard form of the hypergeometric equation by redefining the field $R_\ell(z) = z^{-\ell}(1-z)^2 u_\ell(z)$ and introducing $x = z^2$,

$$u_\ell''(x) + \left(\frac{3}{-1+x} + \frac{1-2\ell}{2x} \right) u_\ell'(x) + \left(-\frac{3(-1+\ell)}{2(-1+x)} + \frac{3(-1+\ell)}{2x} \right) u_\ell(x) = 0 . \quad (5.11)$$

This equation has two linearly independent solutions

$$u_\ell^1(x) = {}_2F_1 \left(\frac{3}{2}, 1-\ell, \frac{1}{2}-\ell, x \right) , \quad u_\ell^2(x) = x^{\frac{2\ell+1}{2}} {}_2F_1 \left(\frac{3}{2}, 2+\ell, \frac{3}{2}+\ell, x \right) . \quad (5.12)$$

For physical values $\ell \in \mathbb{N}$, only the first solution is regular at the horizon $x = 1$. The full solution then is a polynomial of order ℓ ,

$$\begin{aligned} R_\ell^{\text{full}}(z) &= z^{-\ell}(1-z)^2 {}_2F_1 \left(\frac{3}{2}, 1-\ell, \frac{1}{2}-\ell, z^2 \right) \\ &= z^{-\ell}(1-z)^2 \sum_{n=0}^{\ell-1} (-1)^n \binom{\ell-1}{n} \frac{\left(\frac{3}{2}\right)_n}{\left(\frac{1}{2}-\ell\right)_n} z^{2n} . \end{aligned} \quad (5.13)$$

This tells us that there are no logarithmic corrections at $2\ell+1$ PN order and the Love numbers vanish identically. Indeed, matching the one-point functions in the EFT and the full theory we get

$$c_{2\ell+1} \log(r\mu) - m^{-2\ell-1} \frac{(2\ell-1)!!}{4\pi} \lambda_\ell^{s=1}(\mu) \equiv 0 , \forall r > 0 . \quad (5.14)$$

Since the renormalized Love number is a coupling constant on the worldline, it could only depend on the renormalization scale μ and does not depend on r . This implies that

$$c_{2\ell+1} = 0, \quad \lambda_\ell^{s=1}(\mu) = 0 . \quad (5.15)$$

This confirms the computation shown in the specific examples in Section 4.4 that the $2\ell+1$ PN order gravitational nonlinear correction vanishes, and the Love number has no RG running behavior. Thus, the vanishing of the $(2\ell+1)$ PN term in the full theory tells us that the gravitational nonlinear correction $c_{2\ell+1}$ and the Love number λ_ℓ vanish altogether.

Spin-0/2

The argument is similar for the spin-0 and spin-2 perturbations. Introducing $R(z) = z^{-\ell}u(z)$ and $x = z^2$, we rewrite Eq. (5.2) as

$$u''(x) + \left(\frac{1}{-1+x} + \frac{1-2\ell}{2x} \right) u'(x) + \left(\frac{\ell}{2-2x} + \frac{\ell}{2x} \right) u(x) = 0 . \quad (5.16)$$

This equation admits two linearly independent solutions

$$u_1(x) = {}_2F_1 \left(\frac{1}{2}, -\ell, \frac{1}{2} - \ell, x \right), \quad u_2(x) = x^{\frac{2\ell+1}{2}} {}_2F \left(\frac{1}{2}, 1 + \ell, \frac{3}{2} + \ell, x \right) \quad (5.17)$$

For $\ell \in \mathbb{N}$, only $u_1(x)$ is regular at event horizon $x = 1$. Thus, the full theory solution is

$$R_\ell^{\text{full}}(z) = z^{-\ell} {}_2F_1 \left(\frac{1}{2}, -\ell, \frac{1}{2} - \ell, z^2 \right) . \quad (5.18)$$

This is a polynomial of order ℓ , which fully coincides with the result of the EFT PN calculations. Matching this to the full EFT calculation including finite-size effects, we obtain that the Love numbers vanish identically,

$$\lambda_\ell^{s=0} = 0, \quad \lambda_\ell^{s=2} = 0 . \quad (5.19)$$

All in all, we have shown that the worldline EFT approach allows one to unambiguously separate the source and response components of external fields in the response problem in full general relativity. In particular, we have shown that the $(2\ell + 1)$ PN corrections to the source profiles vanish, which implies the absence of RG running of Love numbers. The Love numbers vanish as well, so our final results can be represented in the following diagrammatic form:

$$\sum_{\text{all possible diagrams}} 2\ell + 1 = 0, \quad \lambda_\ell = 0 . \quad (5.20)$$

5.3 Analytic Continuation

For completeness, let us match the Love numbers for the spin-0 case using the analytic continuation prescription. This prescription amounts to treating multipole orbital numbers as rational numbers, $\ell \in \mathbb{R}$. This approach is motivated by higher-dimensional black hole perturbation theory, where the relevant parameter in perturbation equations is $\ell/(d-3)$, where d is the number of spacetime dimensions [16].

For a generic ℓ neither of the two solutions $u_1(x)$ and $u_2(x)$ in Eq.(5.17) is regular at the event horizon $x = 1$. Instead, one obtains a regular solution by combining the two,

$$\begin{aligned} u_\ell(x) &= \frac{\Gamma(\frac{1}{2} + \ell)}{\Gamma(\ell + 1) \Gamma(\frac{1}{2})} {}_2F_1 \left(\frac{1}{2}, -\ell, \frac{1}{2} - \ell, x \right) + \frac{\Gamma(-\frac{1}{2} - \ell)}{\Gamma(\frac{1}{2}) \Gamma(-\ell)} x^{\frac{2\ell+1}{2}} {}_2F \left(\frac{1}{2}, 1 + \ell, \frac{3}{2} + \ell, x \right) \\ &= {}_2F_1 \left(\frac{1}{2}, -\ell, 1, 1 - x \right) . \end{aligned} \quad (5.21)$$

The corresponding full theory solution then reads

$$R_\ell^{\text{full}}(z) = z^{-\ell} {}_2F_1\left(\frac{1}{2}, -\ell, 1, 1 - z^2\right). \quad (5.22)$$

Now, we keep ℓ generic and do the asymptotic expansion of the full theory solution at the asymptotic infinity,

$$\begin{aligned} \lim_{r \rightarrow \infty} R_\ell^{\text{full}}(r) \propto r^\ell \left(1 + c_1 \left(\frac{M}{2r}\right) + c_2 \left(\frac{M}{2r}\right)^2 + \cdots + c_{N_m} \left(\frac{M}{2r}\right)^{N_m} + \cdots \right) \\ + r^{-\ell-1} \left(-\left(\frac{M}{2}\right)^{2\ell+1} \frac{\Gamma(\frac{1}{2}-\ell)\Gamma(1+\ell)}{\Gamma(-\ell)\Gamma(\frac{3}{2}+\ell)} + \cdots \right), \end{aligned} \quad (5.23)$$

where c_1, c_2, \dots are the coefficients given in Eq. (5.5). For generic noninteger and non-half-integer ℓ , the first series describes the PN correction to the source r^ℓ , while the second series describes the BH response. Importantly, these two asymptotic series never mix. This is a celebrated success of the analytic continuation.

Now we take the physical limit $\ell \in \mathbb{N}$. The source series then exactly reduces to our results obtained with the diagrammatic method. The response part, however, vanishes since $\Gamma(-\ell) \rightarrow \infty$ when $\ell \in \mathbb{N}$.

6 Dissipation Numbers

One can extract the dissipation number by matching one-point functions in the EFT and UV theories. In this section we perform this matching explicitly. Importantly, this procedure gives the same dissipation numbers as a matching of absorption cross sections. This is a valuable consistency check of the EFT approach.

To match the dissipation numbers, we solve the time-dependent Teukolsky equation in the near zone approximation. Note that the near zone approximation does not exactly correspond to a low-frequency expansion [20, 22]. As a result, the near zone approximation does not correctly reproduce the time-dependent conservative effects [20]. However, it is sufficient for the matching of the dissipation number, and hence it is adequate for our purposes.

6.1 Near Horizon Teukolsky Equation

The near horizon approximation is based on the fact that the Teukolsky equation simplifies drastically in the regime

$$\omega r \ll 1, \quad M\omega \ll 1. \quad (6.1)$$

Under these assumptions, the spin- s Teukolsky equation can be truncated as (see Appendix E)

$$\begin{aligned} R_\ell''(r) + \left(-\frac{2+4s}{M-2r} - \frac{2s}{r} + \frac{2+4s}{M+2r} \right) R_\ell'(r) \\ + \left(\frac{(s-\ell)(1+s+\ell)}{r^2} + \frac{128M^3\omega(-is+2M\omega)}{(4r^2-M^2)^2} \right) R_\ell(r) = 0. \end{aligned} \quad (6.2)$$

Note that this equation enjoys an $\text{SL}(2, \mathbb{R})$ near horizon symmetry [22].

The physical frequency dependent solution has the ingoing boundary condition at the black hole horizon [54, 74],

$$R_\ell(r) = \text{const} \times \left(r - \frac{M}{2}\right)^{-4iM\omega - 2s}, \quad r \rightarrow \frac{M}{2}. \quad (6.3)$$

Using the field redefinition $R_\ell(z) = z^{s-\ell}(1-z^2)^{-4iM\omega-2s}u_\ell(z)$ and introducing a new variable $x = z^2 = M^2/(4r^2)$ we get

$$\begin{aligned} u_\ell''(x) + \left(\frac{1-2\ell}{2x} + \frac{1-2s-8iM\omega}{-1+x}\right) u_\ell'(x) \\ + \left(\frac{(s+\ell+4iM\omega)(-1+2s+8iM\omega)}{2(-1+x)} - \frac{(s+\ell+4iM\omega)(-1+2s+8iM\omega)}{2x}\right) u_\ell(x) = 0. \end{aligned} \quad (6.4)$$

This equation has two linearly independent solutions

$$\begin{aligned} u_\ell^1(x) &= {}_2F_1\left(\frac{1}{2} - s - 4iM\omega, -s - \ell - 4iM\omega, \frac{1}{2} - \ell, x\right), \\ u_\ell^2(x) &= x^{\frac{2\ell+1}{2}} {}_2F_1\left(\frac{1}{2} - s - 4iM\omega, 1 - s + \ell - 4iM\omega, \frac{3}{2} + \ell, x\right). \end{aligned} \quad (6.5)$$

For $\ell \in \mathbb{N}, s \in \mathbb{N}$ and nonzero ω , only the linear combination of these two solutions is regular at the horizon,

$$\begin{aligned} u_\ell(x) &= {}_2F_1\left(\frac{1}{2} - s - 4iM\omega, -s - \ell - 4iM\omega, 1 - 2s - 8iM\omega, 1 - x\right) \\ &= \frac{\Gamma\left(\frac{1}{2} + \ell\right) \Gamma(1 - 2s - 8iM\omega)}{\Gamma\left(\frac{1}{2} - s - 4iM\omega\right) \Gamma(1 - s + \ell - 4iM\omega)} {}_2F_1\left(\frac{1}{2} - s - 4iM\omega, -s - \ell - 4iM\omega, \frac{1}{2} - \ell, x\right) \\ &\quad + \frac{\Gamma\left(-\frac{1}{2} - \ell\right) \Gamma(1 - 2s - 8iM\omega)}{\Gamma\left(\frac{1}{2} - s - 4iM\omega\right) \Gamma(-s - \ell - 4iM\omega)} \\ &\quad \times x^{\frac{2\ell+1}{2}} {}_2F_1\left(\frac{1}{2} - s - 4iM\omega, 1 - s + \ell - 4iM\omega, \frac{3}{2} + \ell, x\right). \end{aligned} \quad (6.6)$$

To get the dissipation number we need to read off the coefficient in front of the $\sim r^{-s-\ell-1}$ term in the Taylor expansion of R_ℓ . This is particularly easy with our variable choice $x = M^2/(4r^2)$. Indeed, Taylor expansions of the prefactor $(1-z^2)^{-4iM\omega-2s}$ and the first hypergeometric function in the right-hand side of Eq. (6.6) produce only even powers of r , and hence they do not contribute to the $r^{2\ell+1}$ term. This term stems only from the second term (6.6) proportional to $x^{\frac{2\ell+1}{2}}$. Therefore, Taylor expanding (6.6) at $r \rightarrow \infty$, we get

$$R_\ell^{\text{near zone}}(r) \propto r^{\ell-s} \left(1 + \dots + r^{-2\ell-1} \left(i \frac{4(-1)^s(\ell-s)!(\ell+s)!}{(2\ell+1)!!(2\ell-1)!!} M^{2(\ell+1)} \omega\right) + \dots\right). \quad (6.7)$$

We stress that we have not used any analytic continuation in ℓ to obtain the above formula. With our choice of variables, it is obvious that there is no source/response mixing in the full solution. Shortly we will give a simple EFT argument of why the source/response mixing at order $r_s\omega$ is absent in many popular gauges.

6.2 Dissipation Number Matching

Now we can match the EFT one-point function correction due to the dissipation number (2.33) and the UV result (6.7). Note that this matching is actually completely unambiguous in the isotropic gauge, because the finite-frequency PN corrections are proportional to ω^2 . Thus, linear in ω terms unambiguously correspond to the finite-size dissipation contributions. In other words, the dissipation diagram cannot be canceled by any source corrections at the $2\ell + 1$ order PN level in the isotropic gauge.

Now we can do the matching easily. In the spin-0 case, the Teukolsky variable $\psi^{[0]} = \Phi$, with the Feynman rules provided in Appendix A, we can get the spin-0 dissipation number

$$\lambda_{\ell(\omega)}^{s=0} = \frac{8\pi(\ell!)^2}{(2\ell+1)!!((2\ell-1)!!)^2} M^{2\ell+1}. \quad (6.8)$$

In the spin-1 case, the Teukolsky variable $\psi^{[\pm 1]}$ is functions of the Maxwell-Newman-Penrose scalars Φ_0, Φ_1 and Φ_2 [72, 73]

$$\Phi_0 = F_{\mu\nu} l^\mu m^\nu, \quad \Phi_1 = \frac{1}{2} F_{\mu\nu} (l^\mu n^\nu + \bar{m}^\mu m^\nu), \quad \Phi_2 = F_{\mu\nu} \bar{m}^\mu n^\nu. \quad (6.9)$$

In the isotropic coordinates, it is more convenient to work with the rescaled scalars

$$\tilde{\Phi}_0 = \Phi_0, \quad \tilde{\Phi}_1 = \frac{(M+2r)^4}{64M^2r^2} \Phi_1, \quad \tilde{\Phi}_2 = \frac{(M+2r)^4}{64M^2r^2} \Phi_2. \quad (6.10)$$

The Teukolsky variables in this formalism take the form $\psi^{[1]} = \tilde{\Phi}_0$, $\psi^{[-1]} = \tilde{\Phi}_2$. To match the spin-1 dissipation number it is sufficient to use $\psi^{[1]}$,

$$\psi^{[1]} = 2\sqrt{2} \frac{r}{(M-2r)^2} \eth^0 A_0, \quad (6.11)$$

where \eth^0 is the spin raising operator defined in Appendix B.1. This simplification appears because the electric and magnetic fields are clearly separated in $\psi^{[1]}$, so we can set the magnetic source to zero. In this case the real part of $\psi^{[1]}$ is sourced by the electric field and hence entirely by A_0 (see Appendix E.3 for more detail). With the Feynman rules provided in Appendix A, we get the spin-1 electric dissipation number

$$\lambda_{\ell(\omega)}^{s=1} = \frac{8\pi(\ell-1)!(\ell+1)!}{(2\ell+1)!!((2\ell-1)!!)^2} M^{2\ell+1}. \quad (6.12)$$

In the spin-2 electric case, the Weyl scalar $\psi^{[2]} = \psi_0$ is sourced, at the leading order, by the perturbation of the Newtonian potential $\delta\phi$, see (4.39). Since we focus on the parity even sector, the magnetic contributions to the Weyl scalar can be ignored. The responses from other parity-even metric fluctuations only appear at higher orders in the distance expansion, and hence can be ignored when calculating the Weyl scalar in the EFT. Hence, matching the EFT and the GR expressions we get

$$\lambda_{\ell(\omega)}^{s=2} = \frac{8\pi(\ell-2)!(\ell+2)!}{(2\ell+1)!!((2\ell-1)!!)^2} M^{2\ell+1}. \quad (6.13)$$

All together, these results can be combined in a master formula for a generic spin- s field,

$$\lambda_{1(s)}^{\text{non-loc.}} = \frac{8\pi(\ell-s)!(\ell+s)!}{(2\ell+1)!!((2\ell-1)!!)^2\ell!2^{2\ell+1}} r_s^{2\ell+1}, \quad (6.14)$$

where we used (2.34) and expressed the result in terms of the Schwarzschild radius $r_s = 2M$. This expression coincides with the dissipation numbers extracted from the absorption cross sections for $\ell = s$; see Eq. (2.25).

6.3 On Cancellations of Dissipative Response in Advanced Coordinates

In Section 3.3 we have shown that individual static PN diagrams always produce logarithmic divergences at the $(2\ell+1)$ PN order. These logs then cancel after all diagrams are summed over. The situation is different at $\mathcal{O}(\omega r_s)$, where gravitational nonlinear corrections are absent in most gauges. Indeed, in Schwarzschild, isotropic, and harmonic coordinates, the Schwarzschild metric is diagonal in time, which means that any finite frequency interaction is quadratic in frequency, and has the typical form $g^{00}\partial_t\Phi\partial_t\Phi \propto \omega^2$. Thus, at $\mathcal{O}(r_s\omega)$, there is no source/response mixing, and hence there is no ambiguity in the matching procedure.

However, the situation is different in the advanced (Eddington–Finkelstein) coordinates, which have a non-vanishing off-diagonal term g_{0i} [20]. Therefore, in these coordinates we always have the interactions $g^{0i}\partial_t\Phi\partial_i\Phi \propto i\omega$, which can cancel the dissipative response. In the diagrammatic language, the imaginary part of the full theory solution at $2\ell+1.5$ PN order in the advanced coordinates has two distinctive contributions now,

$$\sum_{\text{all possible diagrams}} 2\ell+1 \quad \text{[Diagram: A vertical line with multiple red dots connected by dashed red lines to a central shaded circle labeled } i\omega \text{, which then connects via blue lines to an external point } x \text{ and a crossed circle labeled } r^\ell \text{.]}$$

$$+ \quad Q^b \quad \text{[Diagram: A vertical line with two yellow dots connected by a blue line to an external point } x \text{ and a crossed circle labeled } r^\ell \text{.]} \quad Q^a$$

$$\sim i r^\ell \times \frac{1}{r^{2\ell+1}} \left(A m^{2\ell+2} \omega + \lambda_{\ell(\omega)}(r_s \omega) \right), \quad (6.15)$$

where A is an order-one numerical coefficient. As argued in [20], these two different diagrams must exactly cancel each other out in order to reproduce the full theory calculation in the advanced coordinates. In contrast to the Love number vanishing, this particular cancellation does not represent fine-tuning, as the actual physical dissipative response does not vanish, and can be easily extracted in other gauges. The fact that the cancellation between the $(2\ell+1.5)$ PN graviton corrections and the dissipative response happens only in the advanced coordinates suggests that this cancellation is merely a gauge artifact. Indeed, the physical dissipation is not zero and has a scaling consistent with the Wilsonian naturalness principle; cf. (6.14).

An interesting implication of this argument is that the source/response mixing should generally be present for Kerr BHs. Indeed, the Kerr metric has nonvanishing off-diagonal components in any coordinate system. This is the reason why the Kerr Love response coefficients' calculation is obscured by the source/response mixing [20]. Although the analytic continuation prescription allows one to correctly extract the response coefficients, we believe that any robust analysis should be based on using the EFT. We leave a detailed EFT calculation of the Kerr response coefficients for future work.

7 Conclusions and Outlook

We have computed the EFT one-point functions of static scalar, photon, and graviton perturbations of four-dimensional Schwarzschild black holes. We developed a diagrammatic expansion that computes post-Newtonian corrections to the external field sources. Using the isotropic Kaluza-Klein gauge, we have explicitly resummed the EFT PN diagrams to an arbitrary PN order in the case of spin-0 and spin-2 dilaton fluctuations. These results are valid for any multipolar index ℓ . For the Maxwell field we have obtained explicit results for the $\ell = 1$ case, i.e., at the 3PN order.

Comparing our results with the full BH perturbation theory calculations we have found that the static PN one-point functions explicitly reproduce the full general relativity results without having to include any finite-size effects. This implies that Love numbers vanish identically.

In the second part of our paper we have matched the Schwarzschild BH dissipation numbers. Using the in-in approach we have computed the dissipative corrections to the one-point functions and extracted the dissipation numbers by comparing our EFT field profiles to the general relativity results. Our expressions for the dissipation numbers exactly coincide with the results of matching in a gauge-invariant manner obtained by comparing cross sections for the absorption of massless particles by black holes versus the absorption cross sections in the point-particle theory.

We have also obtained some important results clarifying the EFT description of black holes. At the conceptual level, we have shown how the EFT resolves the so-called source/response ambiguity. Using the EFT we can extract the finite-size effects without having to use the so-called analytic continuation prescription. The second important result is that the individual EFT diagrams generically produce logarithmic corrections to Love numbers. These corrections, however, cancel when all diagrams of the $(2\ell + 1)$ PN order are summed over. We interpret this apparent fine-tuning as a manifestation of the Love symmetry of BH perturbations [22]. The third important result is a consistent definition of dissipation numbers in the EFT, and their explicit relation to the absorption cross sections.

We have also obtained some new results at the technical level, which will be useful in future studies of BH within the worldline EFT formalism. First, we have defined a notion of a consistent gauge that allows for unambiguous matching. Second, we have set up an EFT diagrammatic expansion for external probes and studied its topological properties. Our analysis facilitates the resummation of Feynman diagrams at high PN orders. Key to this resummation is the diagrammatic recurrence relation between PN diagrams of different orders. This recurrence relation is, essentially, the diagrammatic version of the recurrence relation that appears in the Frobenius solution to the Teukolsky equation. Thus, one can use it to systematically resum the EFT diagrams and in this way to recover the entire static solution to the Teukolsky equation that includes all necessary relativistic corrections.

Our study can be extended in multiple ways. First, it will be important to include BH spin and generalize our EFT PN expansion to the case of Kerr black holes along the lines of [9, 34, 59]. Although the Kerr BH Love numbers were shown to vanish [19, 20], these results relied on the analytic continuation prescription, whose validity is not completely warranted. Another project in this research direction would be an explicit matching of dissipation numbers for Kerr black holes, which do not vanish even for static external perturbations. The second potential line of research is to better understand the nature of fine-tuning in the EFT PN expansion. This fine-tuning includes

the cancellation of logarithmic corrections to static Love numbers. In four dimensions this can be explained as a result of the Love symmetry, which enforces the polynomial structure of one-point functions. It would be interesting to study higher-dimensional BHs in the EFT framework and see how the Love symmetry manifests itself there. Finally, it will be important to extract the Love numbers in a fully gauge-invariant manner by comparing the elastic scattering cross sections of external fields off the BH geometry against the EFT on-shell scattering amplitudes (see [39] for recent progress). We leave these research directions for future work.

Acknowledgements We are grateful to Panos Charalambous, Horng Sheng Chia, Sergei Dubovsky, Gregor Kälin, Barak Kol, Rafael A. Porto, Michael Smolkin, and Matias Zaldarriaga for their comments on the draft and enlightening discussions. We also thank Mengyang Zhang for useful discussions. Z.Z. thanks the long term hospitality of the Institute for Advanced Study.

A Feynman Rules

In this section we present Feynman rules for the EFT diagrammatic computation. We work in the isotropic gauge of the background gravitational field. Since the spin-2 electric perturbations share the same structure with the spin-0 perturbations, we only provide the related Feynman rules for the spin-0 case.

Gravitational Sector:

- Propagators:

$$\text{---}\overset{\phi}{\text{---}}\text{---} = 4\pi G \frac{-i}{k^2}, \quad \text{~~~~~}\overset{\sigma}{\text{~~~~~}}\text{~~~~~} = -16\pi G \frac{-i}{k^2} \quad (\text{A.1})$$

- Static vertices:

Worldline vertex:

$$\text{||}\overset{\phi}{\text{---}}\text{---} = -im, \quad (\text{A.2})$$

Bulk vertices:

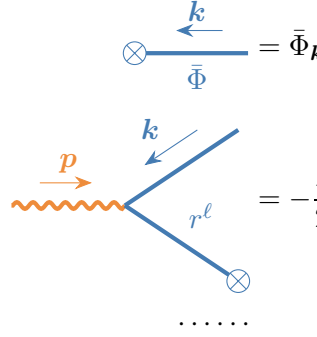
$$\begin{aligned} \text{---}\overset{k}{\text{---}}\text{---} \text{---}\overset{p}{\text{---}}\text{---} \text{~~~~~} &= i \frac{1}{8\pi} \mathbf{k} \cdot \mathbf{p}, \\ \text{~~~~~}\overset{k_1}{\text{~~~~~}} \text{~~~~~} \overset{k_3}{\text{~~~~~}} \text{~~~~~} \overset{k_2}{\text{~~~~~}} &= i \frac{3}{32\pi} (\mathbf{k}_1 \cdot \mathbf{k}_2 + \mathbf{k}_2 \cdot \mathbf{k}_3 + \mathbf{k}_3 \cdot \mathbf{k}_1) \\ &\dots\dots \end{aligned} \quad (\text{A.3})$$

Spin-0 Perturbations:

- Propagator:

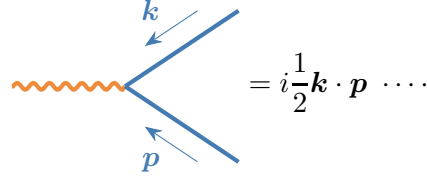
$$\text{---}\overset{\delta\Phi}{\text{---}}\text{---} = \frac{-i}{k^2}. \quad (\text{A.4})$$

- Source vertices:



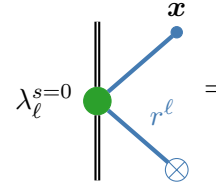
$$= -\frac{\ell}{2} k^i \mathcal{E}_{i i_2 \dots i_\ell} (2\pi)^3 \left(i^{\ell-1} \frac{d^{\ell-1}}{dk_{i_2} \dots dk_{i_\ell}} \delta^{(3)}(\mathbf{k} + \mathbf{p}) \right) \quad (\text{A.5})$$

- Bulk vertices:



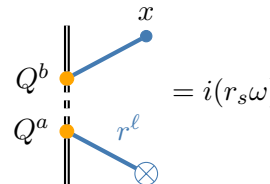
$$= i \frac{1}{2} \mathbf{k} \cdot \mathbf{p} \dots \quad (\text{A.6})$$

- Love number vertex:



$$= \frac{(2\ell - 1)!!}{4\pi} \lambda_\ell^{s=0} \mathcal{E}_{i_1 \dots i_\ell} x^{i_1} \dots x^{i_\ell} \frac{1}{r^{2\ell+1}} . \quad (\text{A.7})$$

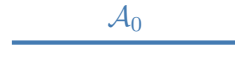
- Dissipation nonlocal vertex:



$$= i(r_s \omega) \frac{(2\ell - 1)!!}{4\pi} \lambda_{\ell(\omega)}^{s=0} \mathcal{E}_{i_1 \dots i_\ell} x^{i_1} \dots x^{i_\ell} \frac{1}{r^{2\ell+1}} e^{-i\omega t} . \quad (\text{A.8})$$

Spin-1 Electric Perturbations:

- Propagator:



$$= (-1) \frac{-i}{\mathbf{k}^2} . \quad (\text{A.9})$$

- Source vertices:

$$\begin{aligned}
& \text{Diagram: A blue line with a circle containing a cross at the left end, labeled } \bar{\mathcal{A}}_0 \text{ below and } \mathbf{k} \text{ above with an arrow pointing left.} \\
& \quad = \bar{\mathcal{A}}_{0\mathbf{k}}, \\
& \text{Diagram: An orange wavy line with an arrow labeled } \mathbf{p} \text{ pointing right, meeting a blue line with an arrow labeled } \mathbf{k} \text{ pointing down-left. The blue line continues to a circle with a cross. The vertex is labeled } r^\ell. \\
& \quad = \frac{\ell}{2} k^i \mathcal{E}_{ii_2 \dots i_\ell} (2\pi)^3 \left(i^{\ell-1} \frac{d^{\ell-1}}{dk_{i_2} \dots dk_{i_\ell}} \delta^{(3)}(\mathbf{k} + \mathbf{p}) \right) \\
& \text{Diagram: A red dashed line with an arrow labeled } \mathbf{p} \text{ pointing right, meeting a blue line with an arrow labeled } \mathbf{k} \text{ pointing down-left. The blue line continues to a circle with a cross. The vertex is labeled } r^\ell. \\
& \quad = -2\ell k^i \mathcal{E}_{ii_2 \dots i_\ell} (2\pi)^3 \left(i^{\ell-1} \frac{d^{\ell-1}}{dk_{i_2} \dots dk_{i_\ell}} \delta^{(3)}(\mathbf{k} + \mathbf{p}) \right) \\
& \quad \dots\dots
\end{aligned} \tag{A.10}$$

- Bulk vertices:

$$\begin{aligned}
& \text{Diagram: An orange wavy line meeting a blue line with an arrow labeled } \mathbf{k} \text{ pointing down-left and another blue line with an arrow labeled } \mathbf{p} \text{ pointing down-right.} \\
& \quad = -i \frac{1}{2} \mathbf{k} \cdot \mathbf{p}, \\
& \text{Diagram: A red dashed line meeting a blue line with an arrow labeled } \mathbf{k} \text{ pointing down-left and another blue line with an arrow labeled } \mathbf{p} \text{ pointing down-right.} \\
& \quad = i 2 \mathbf{k} \cdot \mathbf{p} \dots\dots
\end{aligned} \tag{A.11}$$

- Love number vertex:

$$\begin{aligned}
& \text{Diagram: A green circle with a blue line with an arrow labeled } \mathbf{x} \text{ pointing up-right and another blue line with an arrow labeled } r^\ell \text{ pointing down-right to a circle with a cross. A vertical double line passes through the green circle.} \\
& \quad \lambda_\ell^{s=1} = -\frac{(2\ell-1)!!}{4\pi} \lambda_\ell^{s=1} \mathcal{E}_{i_1 \dots i_\ell} x^{i_1} \dots x^{i_\ell} \frac{1}{r^{2\ell+1}}.
\end{aligned} \tag{A.12}$$

- Dissipation non-local vertex:

$$\begin{aligned}
& \text{Diagram: A vertical double line with two orange dots labeled } Q^b \text{ (top) and } Q^a \text{ (bottom). A blue line with an arrow labeled } \mathbf{x} \text{ points up-right from } Q^b. Another blue line with an arrow labeled } r^\ell \text{ points down-right from } Q^a \text{ to a circle with a cross.} \\
& \quad = -i(r_s \omega) \frac{(2\ell-1)!!}{4\pi} \lambda_{\ell(\omega)}^{s=1} \mathcal{E}_{i_1 \dots i_\ell} x^{i_1} \dots x^{i_\ell} \frac{1}{r^{2\ell+1}} e^{-i\omega t}.
\end{aligned} \tag{A.13}$$

B Useful Mathematical Relations

B.1 (Spin-Weighted) Spherical Harmonics

(Scalar) Spherical Harmonics: We use the following definition of the (scalar) spherical harmonics:

$$Y_{\ell m}(\theta, \phi) = \frac{(-1)^{\ell + \frac{|m|+m}{2}}}{2^\ell \ell!} \left[\frac{2\ell+1}{4\pi} \frac{(\ell - |m|)!}{(\ell + |m|)!} \right]^{1/2} e^{im\phi} (\sin \theta)^{|m|} \left(\frac{d}{d \cos \theta} \right)^{\ell + |m|} (\sin \theta)^{2\ell}, \tag{B.1}$$

with the parameter range $\ell \geq 0$, $-\ell \leq m \leq \ell$ and ℓ, m are all integers. These harmonics obey the following relations:

$$\Delta_{\mathbb{S}^2} Y_{\ell m} = -\ell(\ell+1)Y_{\ell m}, \quad Y_{\ell m}^*(\theta, \phi) = (-1)^m Y_{\ell(-m)}(\theta, \phi), \quad \int_{\mathbb{S}^2} d\Omega Y_{\ell m} Y_{\ell' m'}^* = \delta_{\ell\ell'} \delta_{mm'}, \quad (\text{B.2})$$

where $\Delta_{\mathbb{S}^2}$ is the two-sphere Laplacian.

With the spherical harmonics, we can represent the scalar field contracted between STF tensor \mathcal{E}_L and ℓ copies of normal vector n^L with the spherical harmonic basis

$$n^L(\theta, \varphi) \mathcal{E}_L = \sum_{m=-\ell}^{\ell} \mathcal{E}_{\ell m} Y_{\ell m}(\theta, \varphi), \quad \text{where} \quad \mathcal{E}_{\ell m} = \mathcal{E}_L \int_{\mathbb{S}^2} n^L Y_{\ell m}^* d\Omega. \quad (\text{B.3})$$

This is equivalent to say

$$\mathcal{E}_{i_1 \dots i_\ell} x^{i_1} \dots x^{i_\ell} = \sum_{m=-\ell}^{\ell} \mathcal{E}_{\ell m} r^\ell Y_{\ell m}(\theta, \phi). \quad (\text{B.4})$$

Spin-Weighted Spherical Harmonics: To study the spin-1 and spin-2 perturbations, it is useful to review basic properties of spin-weighted spherical harmonics. We introduce the spin raising and lowering operator

$$\bar{\partial}^s \equiv -\left(\partial_\theta + \frac{i}{\sin \theta} \partial_\phi - s \frac{\cos \theta}{\sin \theta}\right), \quad \bar{\partial}^s \equiv -\left(\partial_\theta - \frac{i}{\sin \theta} \partial_\phi + s \frac{\cos \theta}{\sin \theta}\right), \quad (\text{B.5})$$

with raising and lowering operation

$$\begin{aligned} \bar{\partial}^s ({}_s Y_{\ell m}) &= +\sqrt{(\ell-s)(\ell+s+1)} {}_{s+1} Y_{\ell m}, \\ \bar{\partial}^s ({}_s Y_{\ell m}) &= -\sqrt{(\ell+s)(\ell-s+1)} {}_{s-1} Y_{\ell m}, \end{aligned} \quad (\text{B.6})$$

where $\ell \geq |s|$. Here, ${}_s Y_{\ell m}$ is defined as the spin- s spherical harmonics. These harmonics obey

$${}_s Y_{\ell m}^*(\mathbf{n}) = (-1)^{m+s} {}_{-s} Y_{\ell(-m)}(\mathbf{n}), \quad \int_{\mathbb{S}^2} d\Omega {}_s Y_{\ell m} {}_{\ell' m'}^* = \delta_{\ell\ell'} \delta_{mm'}. \quad (\text{B.7})$$

B.2 Master Integrals

Dimensional regularization is widely used in the EFT diagrammatic computation. In this appendix, we summarize the useful d -dimensional momentum integration and Fourier transforma-

tion formula [38]. The momentum integration formula

$$J = \int \frac{d^d \mathbf{q}}{(2\pi)^d} \frac{1}{(\mathbf{q}^2)^\alpha [(\mathbf{q} + \mathbf{k})^2]^\beta} = \frac{(\mathbf{k}^2)^{d/2-\alpha-\beta}}{(4\pi)^{d/2}} \frac{\Gamma(\alpha + \beta - d/2)}{\Gamma(\alpha)\Gamma(\beta)} \frac{\Gamma(d/2 - \alpha)\Gamma(d/2 - \beta)}{\Gamma(d - \alpha - \beta)} \quad (\text{B.8})$$

$$J_i = \int \frac{d^d \mathbf{q}}{(2\pi)^d} \frac{q_i}{(\mathbf{q}^2)^\alpha [(\mathbf{q} + \mathbf{k})^2]^\beta} = -\frac{d/2 - \alpha}{d - \alpha - \beta} J k_i \quad (\text{B.9})$$

$$\begin{aligned} J_{ij} &= \int \frac{d^d \mathbf{q}}{(2\pi)^d} \frac{q_i q_j}{(\mathbf{q}^2)^\alpha [(\mathbf{q} + \mathbf{k})^2]^\beta} \\ &= \frac{1}{(4\pi)^{d/2}} \frac{\Gamma(\alpha + \beta - d/2 - 1)}{\Gamma(\alpha)\Gamma(\beta)} \frac{\Gamma(d/2 - \alpha + 1)\Gamma(d/2 - \beta)}{\Gamma(d - \alpha - \beta + 2)} \\ &\quad \times \left[(d/2 - \alpha + 1)(\alpha + \beta - d/2 - 1) k_i k_j + (d/2 - \beta) \frac{\mathbf{k}^2}{2} \delta_{ij} \right] (\mathbf{k}^2)^{d/2-\alpha-\beta} \end{aligned} \quad (\text{B.10})$$

$$\begin{aligned} J_{ijk} &= \int \frac{d^d \mathbf{q}}{(2\pi)^d} \frac{q_i q_j q_k}{(\mathbf{q}^2)^\alpha [(\mathbf{q} + \mathbf{k})^2]^\beta} \\ &= \frac{(\mathbf{k}^2)^{d/2-\alpha-\beta}}{(4\pi)^{d/2}} \frac{\Gamma(\alpha + \beta - d/2 - 1)}{\Gamma(\alpha)\Gamma(\beta)} \frac{\Gamma(d/2 - \alpha + 2)\Gamma(d/2 - \beta)}{\Gamma(d - \alpha - \beta + 3)} \\ &\quad \times \left[-(d/2 - \alpha + 2)(\alpha + \beta - d/2 - 1) k_i k_j k_k + (d/2 - \beta) \frac{\mathbf{k}^2}{2} (\delta_{ij} k_k + \delta_{jk} k_i + \delta_{ik} k_j) \right] \end{aligned} \quad (\text{B.11})$$

$$\begin{aligned} J_{ijkl} &= \int \frac{d^d \mathbf{q}}{(2\pi)^d} \frac{q_i q_j q_k q_l}{(\mathbf{q}^2)^\alpha [(\mathbf{q} + \mathbf{k})^2]^\beta} = \frac{(\mathbf{k}^2)^{d/2-\alpha-\beta}}{(4\pi)^{d/2}} \frac{\Gamma(d/2 - \alpha + 2)\Gamma(d/2 - \beta)}{\Gamma(d - \alpha - \beta + 4)} \\ &\quad \times \frac{\Gamma(\alpha + \beta - d/2 - 2)}{\Gamma(\alpha)\Gamma(\beta)} \left[(d/2 - \beta)(d/2 - \beta + 1) (\delta_{ij} \delta_{kl} + \delta_{ik} \delta_{jl} + \delta_{il} \delta_{jk}) \frac{(\mathbf{k}^2)^2}{4} \right. \\ &\quad + (\delta_{ij} k_k k_l + \delta_{ik} k_j k_l + \delta_{il} k_j k_k + \delta_{jk} k_i k_l + \delta_{jl} k_i k_k + \delta_{kl} k_i k_j) \frac{\mathbf{k}^2}{2} \\ &\quad \times (\alpha + \beta - d/2 - 2)(d/2 - \alpha + 2)(d/2 - \beta) \\ &\quad \left. + k_i k_j k_k k_l (\alpha + \beta - d/2 - 2)(\alpha + \beta - d/2 - 1)(d/2 - \alpha + 2)(d/2 - \alpha + 3) \right] \end{aligned} \quad (\text{B.12})$$

Fourier transformation formula:

$$\int \frac{d^d \mathbf{k}}{(2\pi)^d} \frac{e^{i\mathbf{k} \cdot \mathbf{r}}}{(\mathbf{k}^2)^\alpha} = \frac{1}{(4\pi)^{d/2}} \frac{\Gamma(d/2 - \alpha)}{\Gamma(\alpha)} \left(\frac{\mathbf{r}^2}{4} \right)^{\alpha-d/2} \quad (\text{B.13})$$

$$\int \frac{d^d \mathbf{k}}{(2\pi)^d} \frac{\mathbf{k}_i}{(\mathbf{k}^2)^\alpha} e^{i\mathbf{k} \cdot \mathbf{r}} = i x_i \frac{\Gamma(d/2 - \alpha + 1)}{2(4\pi)^{d/2} \Gamma(\alpha)} \left(\frac{\mathbf{r}^2}{4} \right)^{\alpha-d/2-1} \quad (\text{B.14})$$

$$\int \frac{d^d \mathbf{k}}{(2\pi)^d} \frac{\mathbf{k}_i \mathbf{k}_j}{(\mathbf{k}^2)^\alpha} e^{i\mathbf{k} \cdot \mathbf{r}} = \frac{\Gamma(d/2 - \alpha + 1)}{(4\pi)^{d/2} \Gamma(\alpha)} \left(\frac{\delta_{ij}}{2} + (\alpha - d/2 - 1) \frac{x_i x_j}{\mathbf{r}^2} \right) \left(\frac{\mathbf{r}^2}{4} \right)^{\alpha-d/2-1} \quad (\text{B.15})$$

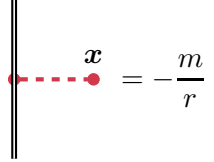
$$\begin{aligned} \int \frac{d^d \mathbf{k}}{(2\pi)^d} \frac{\mathbf{k}_i \mathbf{k}_j \mathbf{k}_l}{(\mathbf{k}^2)^\alpha} e^{i\mathbf{k} \cdot \mathbf{r}} &= \frac{i\Gamma(d/2 - \alpha + 2)}{16(4\pi)^{d/2} \Gamma(\alpha)} \left(\frac{\mathbf{r}^2}{4} \right)^{\alpha-d/2-3} \\ &\quad \times [\mathbf{r}^2 (\delta_{il} x_j + \delta_{jl} x_i + \delta_{ij} x_l) - (d - 2\alpha + 4) x_i x_j x_l] \end{aligned} \quad (\text{B.16})$$

$$\begin{aligned}
\int \frac{d^d \mathbf{k}}{(2\pi)^d} \frac{\mathbf{k}_i \mathbf{k}_j \mathbf{k}_l \mathbf{k}_m}{(\mathbf{k}^2)^\alpha} e^{i\mathbf{k} \cdot \mathbf{r}} &= \frac{\Gamma(d/2 - \alpha + 3)}{32(4\pi)^{d/2} \Gamma(\alpha)} \left(\frac{r^2}{4} \right)^{\alpha - d/2 - 4} \left[(d - 2\alpha + 6) x_i x_j x_l x_m \right. \\
&\quad - r^2 (\delta_{im} x_j x_l + \delta_{jm} x_i x_l + \delta_{lm} x_i x_j + \delta_{il} x_m x_j + \delta_{jl} x_i x_m + \delta_{ij} x_l x_m) \\
&\quad \left. + \frac{(r^2)^2}{(d - 2\alpha + 4)} (\delta_{il} \delta_{jm} + \delta_{jl} \delta_{im} + \delta_{ij} \delta_{lm}) \right] \quad (B.17)
\end{aligned}$$

C Reproducing Schwarzschild Metric at $O((m/r)^4)$

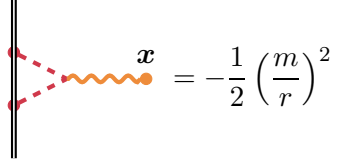
As a consistency check, in this Appendix we show that the graviton one-point function in the EFT can actually reproduce the Schwarzschild metric perturbatively. We have:

- $O((m/r))$:



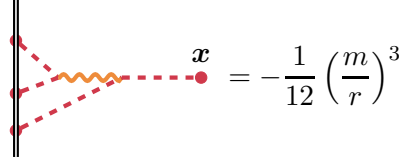
$$x = -\frac{m}{r} . \quad (C.1)$$

- $O((m/r)^2)$:



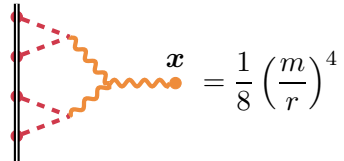
$$x = -\frac{1}{2} \left(\frac{m}{r} \right)^2 . \quad (C.2)$$

- $O((m/r)^3)$:

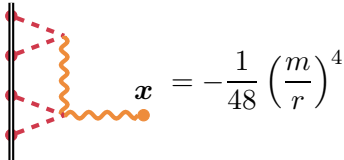


$$x = -\frac{1}{12} \left(\frac{m}{r} \right)^3 . \quad (C.3)$$

- $O((m/r)^4)$:



$$x = \frac{1}{8} \left(\frac{m}{r} \right)^4 . \quad (C.4)$$



$$x = -\frac{1}{48} \left(\frac{m}{r} \right)^4 . \quad (C.5)$$

$$= -\frac{1}{24} \left(\frac{m}{r} \right)^2 . \quad (\text{C.6})$$

After combining all these results, we get the one-point function

$$\phi(\mathbf{x}) = -\frac{m}{r} - \frac{1}{12} \left(\frac{m}{r} \right)^3 , \quad \sigma(\mathbf{x}) = -\frac{1}{2} \left(\frac{m}{r} \right)^2 + \frac{1}{16} \left(\frac{m}{r} \right)^4 . \quad (\text{C.7})$$

Substituting this into Eq.(4.1), we perturbatively derive the metric of Schwarzschild BH in isotropic gauge,

$$g_{00} = 1 - 2 \left(\frac{m}{r} \right) + 2 \left(\frac{m}{r} \right)^2 - \frac{3}{2} \left(\frac{m}{r} \right)^3 + \left(\frac{m}{r} \right)^4 + O \left(\frac{m}{r} \right)^5 , \quad (\text{C.8})$$

$$g_{ij} = \left(1 + 2 \left(\frac{m}{r} \right) + \frac{3}{2} \left(\frac{m}{r} \right)^2 + \frac{1}{2} \left(\frac{m}{r} \right)^3 + \frac{1}{16} \left(\frac{m}{r} \right)^4 + O \left(\frac{m}{r} \right)^5 \right) \delta_{ij} \quad (\text{C.9})$$

D One-point Function of Spin-1 Electric Dipole

In this appendix, we provide the explicit one-point function computation for the spin-1 electric dipole case.

- $O(m/r)$:

$$= \mathcal{E}_i x^i \left(\frac{m}{2r} \right) \times (-2) \quad (\text{D.1})$$

- $O((m/r)^2)$:

$$= \mathcal{E}_i x^i \left(\frac{m}{2r} \right)^2 . \quad (\text{D.2})$$

$$= \mathcal{E}_i x^i \left(\frac{m}{2r} \right)^2 \times (-8) . \quad (\text{D.3})$$

$$= \mathcal{E}_i x^i \left(\frac{m}{2r} \right)^2 \times 8 . \quad (\text{D.4})$$

• $O((m/r)^3)$:

$$= -\mathcal{E}_i x^i \left(\frac{m}{2r}\right)^3 \log(r\mu) \times \frac{4}{3} . \quad (\text{D.5})$$

$$= \mathcal{E}_i x^i \left(\frac{m}{2r}\right)^3 \log(r\mu) \times \frac{28}{3} . \quad (\text{D.6})$$

$$= -\mathcal{E}_i x^i \left(\frac{m}{2r}\right)^3 \log(r\mu) \times \frac{4}{3} . \quad (\text{D.7})$$

$$= \mathcal{E}_i x^i \left(\frac{m}{2r}\right)^3 \log(r\mu) \times 4 . \quad (\text{D.8})$$

$$= -\mathcal{E}_i x^i \left(\frac{m}{2r}\right)^3 \log(r\mu) \times \frac{32}{3} . \quad (\text{D.9})$$

E Teukolsky Equation in Schwarzschild BH

E.1 Equation In Different Coordinates

We derive now the Teukolsky master equation for radial functions in an isotropic coordinate. The full spin- s Teukolsky equation in the Boyer–Lindquist coordinate of Kerr BH for a generic spin- s field reads [74–77]

$$\begin{aligned} & \left[\frac{(r^2 + a^2)^2}{\Delta} - a^2 \sin^2 \theta \right] \frac{\partial^2 \psi^{[s]}}{\partial t^2} + \frac{4Mar}{\Delta} \frac{\partial^2 \psi^{[s]}}{\partial t \partial \phi} + \left[\frac{a^2}{\Delta} - \frac{1}{\sin^2 \theta} \right] \frac{\partial^2 \psi^{[s]}}{\partial \phi^2} \\ & - \Delta^{-s} \frac{\partial}{\partial r} \left(\Delta^{s+1} \frac{\partial \psi^{[s]}}{\partial r} \right) - \frac{1}{\sin \theta} \frac{\partial}{\partial \theta} \left(\sin \theta \frac{\partial \psi^{[s]}}{\partial \theta} \right) - 2s \left[\frac{a(r-M)}{\Delta} + \frac{i \cos \theta}{\sin^2 \theta} \right] \frac{\partial \psi^{[s]}}{\partial \phi} \\ & - 2s \left[\frac{M(r^2 - a^2)}{\Delta} - r - ia \cos \theta \right] \frac{\partial \psi^{[s]}}{\partial t} + (s^2 \cot^2 \theta - s) \psi^{[s]} = 0 , \end{aligned} \quad (\text{E.1})$$

where $\Delta = (r - r_+)(r - r_-)$, $r_+ = M + \sqrt{M^2 - a^2}$, and $r_- = M - \sqrt{M^2 - a^2}$. In the Schwarzschild limit $a = 0$, and in the static limit $\partial_t \rightarrow 0$, we use the variable separation ansatz $\psi^{[s]} = \sum_{\ell m} \mathcal{R}_\ell(r) {}_s Y_{\ell m}(\theta, \phi)$ and get the radial equation in the Schwarzschild coordinates:

$$\mathcal{R}_\ell''(r) + \left(\frac{1+s}{r} + \frac{1+s}{-2M+r} \right) \mathcal{R}_\ell'(r) + \left(-\frac{(s-\ell)(1+s+\ell)}{2Mr} + \frac{(s-\ell)(1+s+\ell)}{2M(-2M+r)} \right) \mathcal{R}_\ell(r) = 0. \quad (\text{E.2})$$

Transforming from the Schwarzschild coordinates to the isotropic coordinates, we get the version of this equation in the isotropic coordinates,

$$\mathcal{R}_\ell''(r) + \left(-\frac{2+4s}{M-2r} - \frac{2s}{r} + \frac{2+4s}{M+2r} \right) \mathcal{R}_\ell'(r) + \frac{(s-\ell)(1+s+\ell)}{r^2} \mathcal{R}_\ell(r) = 0. \quad (\text{E.3})$$

For the finite frequency perturbations in the Schwarzschild background we use the variable separation ansatz $\psi^{[s]} = \sum_{\ell m} \mathcal{R}_\ell(r) {}_s Y_{\ell m}(\theta, \phi) e^{-i\omega t}$, and the corresponding radial equation in the Schwarzschild coordinates reads

$$\begin{aligned} r(r-2M)\mathcal{R}_\ell''(r) + 2(r-M)(1+s)\mathcal{R}_\ell'(r) + \left(s(1+s) - \ell(1+\ell) \right. \\ \left. + 4isr\omega + \frac{-2is\omega r^2(r-M) + r^4\omega^2}{r(r-2M)} \right) \mathcal{R}_\ell(r) = 0. \end{aligned} \quad (\text{E.4})$$

In the near zone region $\omega r \ll 1$, the above equation simplifies:

$$r(r-2M)\mathcal{R}_\ell''(r) + 2(r-M)(1+s)\mathcal{R}_\ell'(r) + \left(s(1+s) - \ell(1+\ell) + \frac{-8isM^3\omega + 16M^4\omega^2}{r(r-2M)} \right) \mathcal{R}_\ell(r) = 0. \quad (\text{E.5})$$

In the isotropic coordinates, the finite frequency radial equation takes the following form:

$$\mathcal{R}_\ell''(r) + \left(-\frac{2+4s}{M-2r} - \frac{2s}{r} + \frac{2+4s}{M+2r} \right) \mathcal{R}_\ell'(r) + \left(\frac{(s-\ell)(1+s+\ell)}{r^2} + \frac{F(\omega, r)}{(4r^2 - M^2)^2} \right) \mathcal{R}_\ell(r) = 0, \quad (\text{E.6})$$

where

$$F(\omega, r) = \frac{(M+2r)^4(8is\omega r(M^2 - 8Mr + 4r^2) + (M+2r)^4\omega^2)}{16r^4}. \quad (\text{E.7})$$

In the near zone region, we use the approximation $F(\omega, M/2) \approx 128M^3\omega(-is + 2M\omega)$.

E.2 Matching Dissipation Number In Schwarzschild Coordinate

Based on the near zone spin- s Teukolsky equation in Schwarzschild coordinate Eq.(E.5), we introduce the following raising and lowering operator to explicitly see the $\text{SL}(2, \mathbb{R})$ symmetry:

$$\begin{aligned} L_1 &= \exp\left(\frac{t}{4M}\right) \left(\Delta^{1/2} \partial_r - 4M(r-M)\Delta^{-1/2} \partial_t + 2(r-M)s\Delta^{-1/2} \right), \\ L_{-1} &= -\exp\left(-\frac{t}{4M}\right) \left(\Delta^{1/2} \partial_r + 4M(r-M)\Delta^{-1/2} \partial_t \right), \\ L_0 &= -4M\partial_t + s, \end{aligned} \quad (\text{E.8})$$

where $\Delta = r(r - 2M)$. These operators obey the $\text{SL}(2, \mathbb{R})$ commutation relations

$$[L_0, L_{\pm 1}] = \mp L_{\pm 1} , \quad [L_1, L_{-1}] = 2L_0 . \quad (\text{E.9})$$

The near zone equation Eq.(E.5) can be written as

$$\mathcal{C}_2 \psi^{[s]} = \ell(\ell + 1) \psi^{[s]} , \quad (\text{E.10})$$

where \mathcal{C}_2 is the quadratic Casimir operator. The ingoing boundary condition at the event horizon in these coordinates takes the form

$$R_\ell(r) = \text{const} \times (r - 2M)^{-2iM\omega - s} , \quad r \rightarrow 2M . \quad (\text{E.11})$$

It is useful to introduce the near zone variable $z = (r - 2M)/2M$ and rewrite Eq.(E.5) as

$$z(1+z)R_\ell''(z) + (1+s)(1+2z)R_\ell'(z) + \left((s-\ell)(1+s+\ell) - \frac{-2isM\omega + 4(M\omega)^2}{z(1+z)} \right) R_\ell(z) = 0 . \quad (\text{E.12})$$

The solution that satisfies the ingoing boundary condition is

$$R_\ell^{\text{full}}(z) = z^{-s/2} (1+z)^{-s/2} P_\ell^{s+4iM\omega}(1+2z) , \quad (\text{E.13})$$

where $P_n^m(z)$ is the associated Legendre function. We perform the asymptotic expansion of R_ℓ^{full} and find that the coefficient in front of the $r^{\ell-s} \times r^{-2\ell-1}$ term is the same as Eq. (6.7). This will lead to the same dissipation number as in Eq. (6.14).

E.3 Comments on Maxwell-Newman-Penrose $\tilde{\Phi}_0$

In this appendix, we show it is sufficient to consider A_0 for the spin-1 dissipation number matching. The Newman-Penrose-Maxwell scalar $\tilde{\Phi}_0$ in Eq.(6.10) takes the following form in the isotropic coordinates:

$$\tilde{\Phi}_0 = 2\sqrt{2} \frac{r}{(M-2r)^2} \left(F_{0\theta} + i \frac{1}{\sin \theta} F_{0\phi} \right) - 8\sqrt{2} \frac{r^3}{(M-2r)(M+2r)^3} \left(F_{r\theta} + i \frac{1}{\sin \theta} F_{r\phi} \right) . \quad (\text{E.14})$$

In the quasi-static approximation we can ignore the temporal components. Let us focus on the magnetic part of the vector potential satisfying $\partial_i A^i = 0$. It is convenient to rewrite it as

$$A_i = \epsilon_{ijk} x^j \partial^k \Psi , \quad (\text{E.15})$$

which is automatically transverse. In the spherical coordinates, the vector potential can be written as

$$\begin{aligned} A_r &= 0 , \quad A_\theta = -r^2 \sin \theta \times r \frac{1}{r^2 \sin^2 \theta} \partial_\phi \Psi = -\frac{r}{\sin \theta} \partial_\phi \Psi , \\ A_\phi &= r^2 \sin \theta \times r \times \frac{1}{r^2} \partial_\theta \Psi = r \sin \theta \partial_\theta \Psi . \end{aligned} \quad (\text{E.16})$$

Plugging this into Eq. (E.14) and taking the long-distance limit, we obtain

$$\tilde{\Phi}_0 \sim \frac{1}{r} \partial^0 (A_0 + i\Psi) . \quad (\text{E.17})$$

This gives us the simplification in the matching procedure because the response of the electric and magnetic fields are separated. When applying the electric source, there is no ambiguity: the real part of the radial function of $\tilde{\Phi}_0$ corresponds to the electric conservative response, i.e., the Love number, while the imaginary part corresponds to the dissipation number.

F Matching Dissipation Numbers From Amplitudes

In this appendix, we compute the EFT absorption cross section for the spin-2 perturbations.

F.1 Fluctuation-dissipation relation

Let us first prove the fluctuation-dissipation theorem for Schwarzschild black holes [44]. To do this, we will use positive and negative frequency Wightman functions defined as

$$\begin{aligned} W_{+L}^{L'}(\tau - \tau') &= \langle Q_L(\tau) Q^{L'}(\tau') \rangle , \\ W_{-L}^{L'}(\tau - \tau') &= \langle Q^{L'}(\tau') Q_L(\tau) \rangle . \end{aligned} \quad (\text{F.1})$$

With this definition, we can easily rewrite the Feynman Green function and the retarded Green functions in terms of Wightman functions,

$$G_{\text{Fey}L}^{L'}(\tau - \tau') = \theta(\tau - \tau') W_{+L}^{L'}(\tau - \tau') + \theta(\tau' - \tau) W_{-L}^{L'}(\tau - \tau') , \quad (\text{F.2})$$

$$G_{\text{ret}L}^{L'}(\tau - \tau') = i\theta(\tau - \tau') \left(W_{+L}^{L'}(\tau - \tau') - W_{-L}^{L'}(\tau - \tau') \right) . \quad (\text{F.3})$$

We assume that Q_L is a Hermitian operator,

$$W_{+L}^{L'}(\tau - \tau')^* = W_{-L}^{L'}(\tau - \tau') , \quad (\text{F.4})$$

and thus

$$\langle T Q_L(\tau) Q^{L'}(\tau') \rangle^* = \langle \bar{T} Q_L(\tau) Q^{L'}(\tau') \rangle , \quad (\text{F.5})$$

where \bar{T} is the anti-time ordering operator. With the above definitions, we can also rewrite the positive frequency Wightman function in terms of the Feynman Green function,

$$W_{+L}^{L'}(\tau - \tau') = \theta(\tau - \tau') G_{\text{Fey}L}^{L'}(\tau - \tau') + \theta(\tau' - \tau) G_{\text{Fey}L}^{L'}(\tau - \tau')^* \quad (\text{F.6})$$

In the frequency space, we will use the dispersive representation

$$G_{\text{ret}L}^{L'}(\omega) = i \int \frac{d\omega'}{2\pi} \frac{W_{+L}^{L'}(\omega') - W_{-L}^{L'}(\omega')}{\omega - \omega' + i\epsilon} . \quad (\text{F.7})$$

After expanding this relation into real and imaginary parts, we get

$$\text{Re} G_{\text{ret}L}^{L'}(\omega) = -\frac{1}{2} \text{Im} \left[W_{+L}^{L'}(\omega) - W_{-L}^{L'}(\omega) \right] - \text{Pr} \int_0^\infty \frac{\omega' d\omega'}{\pi} \frac{\text{Re} \left[W_{+L}^{L'}(\omega') - W_{-L}^{L'}(\omega') \right]}{\omega^2 - \omega'^2} , \quad (\text{F.8})$$

and

$$\text{Im} G_{\text{ret}L}^{L'}(\omega) = \frac{1}{2} \text{Re} \left[W_{+L}^{L'}(\omega) - W_{-L}^{L'}(\omega) \right] - \omega \text{Pr} \int_0^\infty \frac{d\omega'}{\pi} \frac{\text{Im} \left[W_{+L}^{L'}(\omega') - W_{-L}^{L'}(\omega') \right]}{\omega^2 - \omega'^2} . \quad (\text{F.9})$$

Here, we mention clearly that the above equation holds for a generic tensor structure in L and L' . For the special situation of Schwarzschild BHs the tensorial structure consistent with spherical symmetry is only $\delta_{\langle L' \rangle}^{(L)}$, i.e.,

$$W_{+L}^{L'}(\omega) = w_+(\omega) \delta_{\langle L' \rangle}^{(L)} . \quad (\text{F.10})$$

In this case one can show that $W_{+L}^{L'}(\omega)^* = W_{+L}^{L'}(\omega)$, and thus $W_{+L}^{L'}(\omega)$ is real.

Now we make use of Eq. (F.6), and express the positive frequency Wightman function as,

$$\begin{aligned}
W_{+L}^{L'}(\omega) &= \int_0^{+\infty} d\tau e^{i\omega\tau} \langle TQ_L(\tau)Q^{L'}(0) \rangle + \int_{-\infty}^0 d\tau e^{i\omega\tau} \langle TQ_L(\tau)Q^{L'}(0) \rangle^* \\
&= \int_0^{+\infty} d\tau e^{i\omega\tau} \langle TQ_L(\tau)Q^{L'}(0) \rangle + \int_0^{+\infty} d\tau e^{-i\omega\tau} \langle TQ_L(-\tau)Q^{L'}(0) \rangle^* \\
&= \int_0^{+\infty} d\tau e^{i\omega\tau} \langle TQ_L(\tau)Q^{L'}(0) \rangle + \int_0^{+\infty} d\tau e^{-i\omega\tau} \langle TQ_L(0)Q^{L'}(\tau) \rangle^* \\
&= 2\text{Im} \left[i \int_0^{+\infty} d\tau e^{i\omega\tau} \langle TQ_L(\tau)Q^{L'}(0) \rangle \right],
\end{aligned} \tag{F.11}$$

where we have used the translation invariance of the Green function

$$\langle TQ_L(-\tau)Q^{L'}(0) \rangle = \langle TQ_L(0)Q^{L'}(\tau) \rangle, \tag{F.12}$$

and the definition of the Feynman Green function that implies invariance under the exchange of the time argument,

$$\langle TQ_L(\tau)Q^{L'}(0) \rangle = \langle TQ_L(0)Q^{L'}(\tau) \rangle. \tag{F.13}$$

Since we are interested in classical black holes, we assume the Boulware state, so that the response is purely absorptive,

$$w_+(\omega < 0) = 0. \tag{F.14}$$

Thus, for $\omega > 0$ we have from (F.11):

$$0 = W_{+L}^{L'}(-\omega) = 2\text{Im} \left[i \int_0^{+\infty} d\tau e^{-i\omega\tau} \langle TQ_L(\tau)Q^{L'}(0) \rangle \right] = 2\text{Im} \left[i \int_{-\infty}^0 d\tau e^{i\omega\tau} \langle TQ_L(\tau)Q^{L'}(0) \rangle \right], \tag{F.15}$$

which then allows us to complete the integral in (F.11) and finally obtain

$$W_{+L}^{L'}(\omega) = 2\text{Im} \left[i \int_{-\infty}^{+\infty} d\tau e^{i\omega\tau} \langle TQ_L(\tau)Q^{L'}(0) \rangle \right], \quad \omega > 0. \tag{F.16}$$

Now we can establish the relationship between the Feynman and retarded Green functions in the EFT. Using Eq. (F.9) we get

$$\text{Im}G_{\text{ret}L}^{L'}(\omega) = \text{Re}G_{\text{Fey}L}^{L'}(\omega), \tag{F.17}$$

which fixes the odd frequency terms in Eq. (2.15).

F.2 Spin-2 Absorption Cross Section in the EFT

We start with the definition of the electric-type tidal field,

$$E_{ij} = 2\sqrt{2}M_{\text{pl}}C_{0i0j} \simeq -\sqrt{2}M_{\text{pl}}\partial_0^2 h_{ij}. \tag{F.18}$$

The electric part of the absorption cross section can be obtained from the optical theorem: it is given by the imaginary part of the forward amplitude

$$\sigma_{\text{abs}}^E(\omega) = \frac{2}{\omega} \times \frac{1}{2} \times 2\text{Im}i \int d\tau e^{i\omega\tau} \left[\omega^4 \epsilon^{*ij}(\mathbf{k}, h) \epsilon_{kl}(\mathbf{k}, h) \langle TQ_{ij}(\tau) Q^{kl}(0) \rangle \right], \quad (\text{F.19})$$

where $1/\omega$ is the phase space factor and $1/2$ comes from the Taylor expansion of the S-matrix. $\epsilon_{ij}(\mathbf{k}, h)$ above is the polarization tensor. The first factor of 2 comes from the definition of the tidal field (F.18), and the second factor of 2 comes from the symmetry factor of the Feynman diagrams. We choose \mathbf{k}/\hat{z} , and then the polarization tensor takes the form

$$\epsilon_{ij}(\mathbf{k}, \pm 2) = \begin{pmatrix} \frac{1}{2} & \pm \frac{i}{2} & 0 \\ \pm \frac{i}{2} & -\frac{1}{2} & 0 \\ 0 & 0 & 0 \end{pmatrix}. \quad (\text{F.20})$$

Using and the explicit expressions (2.15) and

$$\delta_{\langle ij \rangle}^{\langle kl \rangle} = \frac{1}{2} \left[\delta_i^k \delta_j^l + \delta_i^l \delta_j^k - \frac{2}{3} \delta_{ij} \delta^{kl} \right], \quad (\text{F.21})$$

we find the electric part of the total cross section

$$\sigma_{\text{abs}}^E(\omega) = 4\omega^4 \lambda_1^{\text{non-loc.}}|_{\ell=s=2}, \quad \omega > 0. \quad (\text{F.22})$$

The magnetic part of the total cross section is the same as the electric part thanks to the “electric-magnetic” duality [21, 44, 59] of the Schwarzschild black holes. Thus, the total cross section is given by

$$\sigma_{\text{abs}}(\omega) = 2\sigma_{\text{abs}}^E(\omega) = 8\omega^4 \lambda_1^{\text{non-loc.}}|_{\ell=s=2}. \quad (\text{F.23})$$

References

- [1] **LIGO Scientific, Virgo** Collaboration, B. P. Abbott et al., *Observation of Gravitational Waves from a Binary Black Hole Merger*, *Phys. Rev. Lett.* **116** (2016), no. 6 061102, [[arXiv:1602.03837](#)].
- [2] E. E. Flanagan and T. Hinderer, *Constraining neutron star tidal Love numbers with gravitational wave detectors*, *Phys. Rev. D* **77** (2008) 021502, [[arXiv:0709.1915](#)].
- [3] J. Vines, E. E. Flanagan, and T. Hinderer, *Post-1-Newtonian tidal effects in the gravitational waveform from binary inspirals*, *Phys. Rev. D* **83** (2011) 084051, [[arXiv:1101.1673](#)].
- [4] D. Bini, T. Damour, and G. Faye, *Effective action approach to higher-order relativistic tidal interactions in binary systems and their effective one body description*, *Phys. Rev. D* **85** (2012) 124034, [[arXiv:1202.3565](#)].
- [5] **LIGO Scientific, Virgo** Collaboration, B. P. Abbott et al., *GW170817: Observation of Gravitational Waves from a Binary Neutron Star Inspiral*, *Phys. Rev. Lett.* **119** (2017), no. 16 161101, [[arXiv:1710.05832](#)].
- [6] R. A. Porto, *The Tune of Love and the Nature(ness) of Spacetime*, *Fortsch. Phys.* **64** (2016), no. 10 723–729, [[arXiv:1606.08895](#)].
- [7] W. D. Goldberger and I. Z. Rothstein, *An Effective field theory of gravity for extended objects*, *Phys. Rev. D* **73** (2006) 104029, [[hep-th/0409156](#)].

- [8] W. D. Goldberger, *Les Houches lectures on effective field theories and gravitational radiation*, in *Les Houches Summer School - Session 86: Particle Physics and Cosmology: The Fabric of Spacetime*, 1, 2007. [hep-ph/0701129](#).
- [9] R. A. Porto, *Post-Newtonian corrections to the motion of spinning bodies in NRGR*, *Phys. Rev. D* **73** (2006) 104031, [[gr-qc/0511061](#)].
- [10] R. A. Porto, *The effective field theorist’s approach to gravitational dynamics*, *Phys. Rept.* **633** (2016) 1–104, [[arXiv:1601.04914](#)].
- [11] M. Levi, *Effective Field Theories of Post-Newtonian Gravity: A comprehensive review*, *Rept. Prog. Phys.* **83** (2020), no. 7 075901, [[arXiv:1807.01699](#)].
- [12] W. D. Goldberger, *Effective field theories of gravity and compact binary dynamics: A Snowmass 2021 whitepaper*, in *2022 Snowmass Summer Study*, 6, 2022. [arXiv:2206.14249](#).
- [13] H. Fang and G. Lovelace, *Tidal coupling of a Schwarzschild black hole and circularly orbiting moon*, *Phys. Rev. D* **72** (2005) 124016, [[gr-qc/0505156](#)].
- [14] T. Damour and A. Nagar, *Relativistic tidal properties of neutron stars*, *Phys. Rev. D* **80** (2009) 084035, [[arXiv:0906.0096](#)].
- [15] T. Binnington and E. Poisson, *Relativistic theory of tidal Love numbers*, *Phys. Rev. D* **80** (2009) 084018, [[arXiv:0906.1366](#)].
- [16] B. Kol and M. Smolkin, *Black hole stereotyping: Induced gravito-static polarization*, *JHEP* **02** (2012) 010, [[arXiv:1110.3764](#)].
- [17] P. Landry and E. Poisson, *Tidal deformation of a slowly rotating material body. External metric*, *Phys. Rev. D* **91** (2015) 104018, [[arXiv:1503.07366](#)].
- [18] A. Le Tiec, M. Casals, and E. Franzin, *Tidal Love Numbers of Kerr Black Holes*, *Phys. Rev. D* **103** (2021), no. 8 084021, [[arXiv:2010.15795](#)].
- [19] H. S. Chia, *Tidal deformation and dissipation of rotating black holes*, *Phys. Rev. D* **104** (2021), no. 2 024013, [[arXiv:2010.07300](#)].
- [20] P. Charalambous, S. Dubovsky, and M. M. Ivanov, *On the Vanishing of Love Numbers for Kerr Black Holes*, *JHEP* **05** (2021) 038, [[arXiv:2102.08917](#)].
- [21] L. Hui, A. Joyce, R. Penco, L. Santoni, and A. R. Solomon, *Static response and Love numbers of Schwarzschild black holes*, *JCAP* **04** (2021) 052, [[arXiv:2010.00593](#)].
- [22] P. Charalambous, S. Dubovsky, and M. M. Ivanov, *Hidden Symmetry of Vanishing Love Numbers*, *Phys. Rev. Lett.* **127** (2021), no. 10 101101, [[arXiv:2103.01234](#)].
- [23] L. Hui, A. Joyce, R. Penco, L. Santoni, and A. R. Solomon, *Ladder symmetries of black holes. Implications for love numbers and no-hair theorems*, *JCAP* **01** (2022), no. 01 032, [[arXiv:2105.01069](#)].
- [24] L. Hui, A. Joyce, R. Penco, L. Santoni, and A. R. Solomon, *Near-Zone Symmetries of Kerr Black Holes*, [arXiv:2203.08832](#).
- [25] E. Poisson and C. M. Will, *Gravity: Newtonian, post-newtonian, relativistic*. Cambridge University Press, 2014.
- [26] K. S. Thorne and J. B. Hartle, *Laws of motion and precession for black holes and other bodies*, *Phys. Rev. D* **31** (1984) 1815–1837.
- [27] A. Le Tiec and M. Casals, *Spinning Black Holes Fall in Love*, *Phys. Rev. Lett.* **126** (2021), no. 13

- 131102, [[arXiv:2007.00214](#)].
- [28] S. Mano, H. Suzuki, and E. Takasugi, *Analytic solutions of the Regge-Wheeler equation and the postMinkowskian expansion*, *Prog. Theor. Phys.* **96** (1996) 549–566, [[gr-qc/9605057](#)].
 - [29] S. Mano, H. Suzuki, and E. Takasugi, *Analytic solutions of the Teukolsky equation and their low frequency expansions*, *Prog. Theor. Phys.* **95** (1996) 1079–1096, [[gr-qc/9603020](#)].
 - [30] S. Mano and E. Takasugi, *Analytic solutions of the Teukolsky equation and their properties*, *Prog. Theor. Phys.* **97** (1997) 213–232, [[gr-qc/9611014](#)].
 - [31] V. Cardoso, E. Franzin, A. Maselli, P. Pani, and G. Raposo, *Testing strong-field gravity with tidal Love numbers*, *Phys. Rev. D* **95** (2017), no. 8 084014, [[arXiv:1701.01116](#)]. [Addendum: *Phys.Rev.D* **95**, 089901 (2017)].
 - [32] S. Cai and K.-D. Wang, *Non-vanishing of tidal Love numbers*, [arXiv:1906.06850](#).
 - [33] S. E. Gralla, *On the Ambiguity in Relativistic Tidal Deformability*, *Class. Quant. Grav.* **35** (2018), no. 8 085002, [[arXiv:1710.11096](#)].
 - [34] W. D. Goldberger, J. Li, and I. Z. Rothstein, *Non-conservative effects on spinning black holes from world-line effective field theory*, *JHEP* **06** (2021) 053, [[arXiv:2012.14869](#)].
 - [35] E. Poisson, *Tidal deformation of a slowly rotating black hole*, *Phys. Rev. D* **91** (2015), no. 4 044004, [[arXiv:1411.4711](#)].
 - [36] E. Poisson, *Compact body in a tidal environment: New types of relativistic Love numbers, and a post-Newtonian operational definition for tidally induced multipole moments*, *Phys. Rev. D* **103** (2021), no. 6 064023, [[arXiv:2012.10184](#)].
 - [37] B. Kol and M. Smolkin, *Classical Effective Field Theory and Caged Black Holes*, *Phys. Rev. D* **77** (2008) 064033, [[arXiv:0712.2822](#)].
 - [38] B. Kol and M. Smolkin, *Dressing the Post-Newtonian two-body problem and Classical Effective Field Theory*, *Phys. Rev. D* **80** (2009) 124044, [[arXiv:0910.5222](#)].
 - [39] M. M. Ivanov and Z. Zhou, *Vanishing of black hole tidal Love numbers from scattering amplitudes*, [arXiv:2209.14324](#).
 - [40] P. Charalambous, S. Dubovsky, and M. M. Ivanov, *Love symmetry*, *JHEP* **10** (2022) 175, [[arXiv:2209.02091](#)].
 - [41] R. A. Porto , *private communication*.
 - [42] C. Cheung , *private communication*.
 - [43] L. Hui , *private communication*.
 - [44] W. D. Goldberger and I. Z. Rothstein, *Dissipative effects in the worldline approach to black hole dynamics*, *Phys. Rev. D* **73** (2006) 104030, [[hep-th/0511133](#)].
 - [45] J. Schwinger, *Brownian motion of a quantum oscillator*, *Journal of Mathematical Physics* **2** (1961), no. 3 407–432.
 - [46] P. M. Bakshi and K. T. Mahanthappa, *Expectation value formalism in quantum field theory. i*, *Journal of Mathematical Physics* **4** (1963), no. 1 1–11.
 - [47] P. M. Bakshi and K. T. Mahanthappa, *Expectation value formalism in quantum field theory. 2.*, *J. Math. Phys.* **4** (1963) 12–16.
 - [48] L. V. Keldysh et al., *Diagram technique for nonequilibrium processes*, *Sov. Phys. JETP* **20** (1965),

no. 4 1018–1026.

- [49] R. D. Jordan, *Effective field equations for expectation values*, *Physical Review D* **33** (1986), no. 2 444.
- [50] L. D. Landau, E. Lifshitz, and L. Pitaevskij, *Course of theoretical physics. vol. 10: Physical kinetics*. Oxford, 1981.
- [51] K.-c. Chou, Z.-b. Su, B.-l. Hao, and L. Yu, *Equilibrium and nonequilibrium formalisms made unified*, *Physics Reports* **118** (1985), no. 1-2 1–131.
- [52] F. M. Haehl, R. Loganayagam, and M. Rangamani, *Schwinger-Keldysh formalism. Part I: BRST symmetries and superspace*, *JHEP* **06** (2017) 069, [[arXiv:1610.01940](#)].
- [53] C. R. Galley and M. Tiglio, *Radiation reaction and gravitational waves in the effective field theory approach*, *Phys. Rev. D* **79** (2009) 124027, [[arXiv:0903.1122](#)].
- [54] A. Starobinskii and S. Churilov, *Amplification of electromagnetic and gravitational waves scattered by a rotating black hole*, *Zh. eksp. teor. Fiz* **65** (1973), no. 3 3–11.
- [55] D. N. Page, *Particle emission rates from a black hole. ii. massless particles from a rotating hole*, *Physical Review D* **14** (1976), no. 12 3260.
- [56] J. F. Donoghue, M. M. Ivanov, and A. Shkerin, *EPFL Lectures on General Relativity as a Quantum Field Theory*, [arXiv:1702.00319](#).
- [57] R. Feynman, *Quantum theory of gravitation*, .
- [58] M. J. Duff, *Quantum tree graphs and the schwarzschild solution*, *Physical Review D* **7** (1973), no. 8 2317.
- [59] R. A. Porto, *Absorption effects due to spin in the worldline approach to black hole dynamics*, *Phys. Rev. D* **77** (2008) 064026, [[arXiv:0710.5150](#)].
- [60] K. S. Thorne, *Multipole Expansions of Gravitational Radiation*, *Rev. Mod. Phys.* **52** (1980) 299–339.
- [61] C. Cheung, I. Z. Rothstein, and M. P. Solon, *From Scattering Amplitudes to Classical Potentials in the Post-Minkowskian Expansion*, *Phys. Rev. Lett.* **121** (2018), no. 25 251101, [[arXiv:1808.02489](#)].
- [62] Z. Bern, C. Cheung, R. Roiban, C.-H. Shen, M. P. Solon, and M. Zeng, *Scattering Amplitudes and the Conservative Hamiltonian for Binary Systems at Third Post-Minkowskian Order*, *Phys. Rev. Lett.* **122** (2019), no. 20 201603, [[arXiv:1901.04424](#)].
- [63] C. Cheung and M. P. Solon, *Classical gravitational scattering at $\mathcal{O}(G^3)$ from Feynman diagrams*, *JHEP* **06** (2020) 144, [[arXiv:2003.08351](#)].
- [64] C. Cheung and M. P. Solon, *Tidal Effects in the Post-Minkowskian Expansion*, *Phys. Rev. Lett.* **125** (2020), no. 19 191601, [[arXiv:2006.06665](#)].
- [65] T. Damour, *High-energy gravitational scattering and the general relativistic two-body problem*, *Phys. Rev. D* **97** (2018), no. 4 044038, [[arXiv:1710.10599](#)].
- [66] Z. Bern, J. Parra-Martinez, R. Roiban, E. Sawyer, and C.-H. Shen, *Leading Nonlinear Tidal Effects and Scattering Amplitudes*, *JHEP* **05** (2021) 188, [[arXiv:2010.08559](#)].
- [67] G. Kälin, Z. Liu, and R. A. Porto, *Conservative Dynamics of Binary Systems to Third Post-Minkowskian Order from the Effective Field Theory Approach*, *Phys. Rev. Lett.* **125** (2020), no. 26 261103, [[arXiv:2007.04977](#)].
- [68] D. Bini, T. Damour, and A. Geralico, *Novel approach to binary dynamics: application to the fifth post-Newtonian level*, *Phys. Rev. Lett.* **123** (2019), no. 23 231104, [[arXiv:1909.02375](#)].

- [69] W. D. Goldberger and A. Ross, *Gravitational radiative corrections from effective field theory*, *Phys. Rev. D* **81** (2010) 124015, [[arXiv:0912.4254](#)].
- [70] A. Ross, *Multipole expansion at the level of the action*, *Phys. Rev. D* **85** (2012) 125033, [[arXiv:1202.4750](#)].
- [71] W. Kinnersley, *Type d vacuum metrics*, *Journal of Mathematical Physics* **10** (1969), no. 7 1195–1203.
- [72] E. Newman and R. Penrose, *An approach to gravitational radiation by a method of spin coefficients*, *Journal of Mathematical Physics* **3** (1962), no. 3 566–578.
- [73] E. Newman and R. Penrose, *Errata: an approach to gravitational radiation by a method of spin coefficients*, *Journal of Mathematical Physics* **4** (1963), no. 7 998–998.
- [74] S. A. Teukolsky, *Perturbations of a rotating black hole. i. fundamental equations for gravitational, electromagnetic, and neutrino-field perturbations*, *The Astrophysical Journal* **185** (1973) 635–648.
- [75] S. A. Teukolsky, *Rotating black holes: Separable wave equations for gravitational and electromagnetic perturbations*, *Physical Review Letters* **29** (1972), no. 16 1114.
- [76] W. H. Press and S. A. Teukolsky, *Perturbations of a rotating black hole. ii. dynamical stability of the kerr metric*, *The Astrophysical Journal* **185** (1973) 649–674.
- [77] S. A. Teukolsky and W. Press, *Perturbations of a rotating black hole. iii-interaction of the hole with gravitational and electromagnetic radiation*, *The Astrophysical Journal* **193** (1974) 443–461.